Curie temperatures of synthetic titanomagnetites in the Fe-Ti-O system: Effects of composition, crystal chemistry, and thermomagnetic methods

Dominique Lattard,[1] Ralf Engelmann,[1] Agnes Kontny,[2] and Ursula Sauerzapf[1]

Received 22 June 2006; revised 22 September 2006; accepted 10 October 2006; published 20 December 2006.

[1] The present study is aimed at improving the calibration of the compositional dependence of the Curie temperature (T_C) of titanomagnetite (Tmt) on the basis of temperature-dependent magnetic susceptibility (χ-T) curves measured on synthetic Tmts in the Fe-Ti-O system. In order to assess the possible influence of high-temperature cation vacancies onto the T_C values, we have synthesized two types of assemblages in subsolidus conditions at 1 bar, 1100°C and 1300°C, under controlled oxygen fugacity conditions. Tmts synthesized in equilibrium with ilmenite-hematite$_{ss}$ (Ilm_{ss}) are expected to have the highest vacancy concentrations, those in equilibrium with wüstite (Wus) the lowest. The composition and homogeneity of the synthetic Tmts were carefully checked with a scanning electron microscope (SEM) and an electron microprobe (EMP). T_C was determined from χ-T curves using a kappabridge and, for comparison, from M_s-T curves measured with a variable field translation balance. Our data set shows systematically higher T_C values for Tmt coexisting with Ilm_{ss} than for Tmt coexisting with Wus. Most χ-T curves are nonreversible, whereby the largest ΔT_C (40 K) concern Tmt(+Ilm_{ss}) of intermediate compositions synthesized at 1300°C. Nonreversibility is interpreted as reflecting cation reordering in Tmt during the high-temperature χ-T measurements. T_C values obtained from M_s-T curves are higher than those obtained from the χ-T curves, whereby the difference regularly increases (up to 40 K) with increasing Ti content, up to $X_{Usp} = 0.6$. Our new calibration curves are suitable to retrieve Tmt compositions in basalts that were rapidly cooled and not oxidized by deuteric or hydrothermal fluids.

Citation: Lattard, D., R. Engelmann, A. Kontny, and U. Sauerzapf (2006), Curie temperatures of synthetic titanomagnetites in the Fe-Ti-O system: Effects of composition, crystal chemistry, and thermomagnetic methods, *J. Geophys. Res.*, *111*, B12S28, doi:10.1029/2006JB004591.

1. Introduction

[2] Measurements of the temperature dependence of the AC magnetic susceptibility are increasingly used to identify magnetic minerals, in particular members of the two solid solutions of iron-titanium-oxide minerals, titanomagnetite (Tmt) and ilmenite-hematite (Ilm_{ss}) which are the essential carriers of magnetism in basalts [e.g., *Dunlop and Özdemir*, 1997; *Calvo et al.*, 2002; *Miranda et al.*, 2002]. This method has proven very useful to estimate the chemical composition of titanomagnetite (solid solution between magnetite, Fe_3O_4, and ulvöspinel, $FeTiO_4$), especially in case of crystals that are not measurable with the electron microprobe, because they are very small or skeletal or crowded with fine lamellae of ilmenite or of other spinel phases (see examples of *Haggerty* [1991]). In case of rocks that contain different generations of Tmt, the temperature-dependent susceptibility measurements can help estimate the corresponding different chemical compositions of this phase and reconstruct the crystallization and alteration history of the basaltic rock [e.g., *Zhou et al.*, 2000; *Kontny et al.*, 2003]. The magnetic susceptibility measurements have also the great advantage of being rapid and straightforward and, in principal, nondestructive. They can be performed on very small chunks of rock (a few mg in weight), i.e., without any time-consuming and costly preparation procedure.

[3] Estimates of the chemical composition of Tmt are based on the compositional dependence of the Curie temperature (T_C) first established by *Akimoto et al.* [1957] and confirmed by a wealth of further experimental studies in the Fe-Ti-O system [e.g., *Ozima and Larson*, 1970; *Bleil*, 1973, 1976; *Hauptman*, 1974; *Rahman and Parry*, 1978; *Cisowski*, 1980; *Deutsch et al.*, 1981; *Tucker*, 1981; *Özdemir and O'Reilly*, 1981; *Moskowitz*, 1987, 1993; *Wanamaker and Moskowitz*, 1994; *Dunlop and Özdemir*, 1997; *Moskowitz et al.*, 1998; *Özdemir*, 2000]. All experimental results point to a negative correlation between Curie temperature and ulvöspinel content of the titanomagnetites

[1] Mineralogisches Institut, Universität Heidelberg, Heidelberg, Germany.
[2] Geologisch-paläontologisches Institut, Universität Heidelberg, Heidelberg, Germany.

0148-0227/06/2006JB004591$09.00

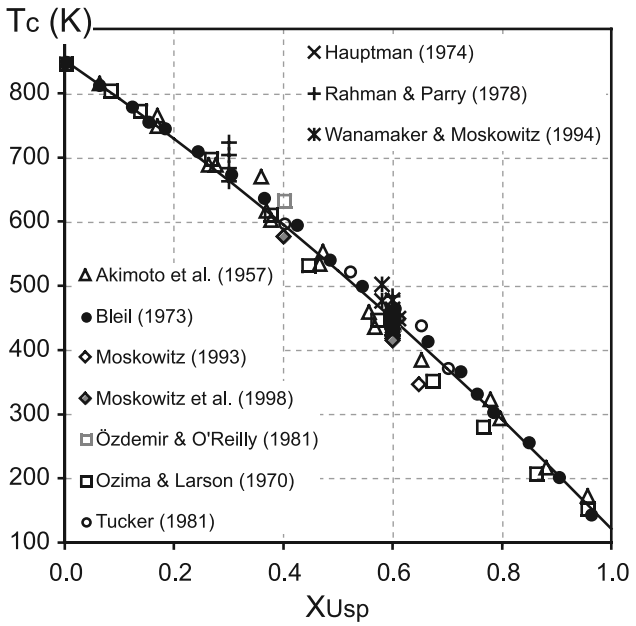

Figure 1. Literature data on the variation of the Curie temperature (T_C) in synthetic titanomagnetites in the Fe-Ti-O system as a function of composition (mole fraction of the ulvöspinel end-member, X_{Usp}). The curve represents the polynomial fit $T_C = -150\,X_{Usp}^2 - 580\,X_{Usp} + 851$ [*Bleil and Petersen*, 1982, p 330].

(Figure 1). Second-order polynomial regression curves have been proposed to estimate the mineral composition from T_C or vice versa (equations reported by *Bleil* [1976], *Bleil and Petersen* [1982, p.330], *Clark* [1997, p. 86], and *Hunt et al.* [1995]; see Figure 1). Because synthetic titanomagnetites with a few wt % Al_2O_3 or MgO display Curie temperatures lower by no more than 40°C [*Richards et al.*, 1973; *O'Donovan and O'Reilly*, 1977; *Özdemir and O'Reilly*, 1978, 1981; *Moskowitz*, 1993], i.e., in rough agreement with the Al- and Mg-free ones, the regression curves appear also applicable to complex, nature-relevant Tmt compositions. Indeed, these curves have been commonly used in rock magnetic and paleomagnetic studies [e.g., *Bücker et al.*, 1986; *Gonzalez et al.*, 1997].

[4] Nevertheless, even for synthetic Tmt in the Fe-Ti-O system, the available literature data on the Curie temperature scatter significantly, allowing only rough estimates of their compositions, with uncertainties around ± 0.1 for the mole fraction of the ulvöspinel end-member. This scattering partially reflects uncertainties concerning the chemical composition of the synthetic titanomagnetites used for calibration. In several studies it is not clear whether the samples were really single-phased and chemically homogeneous because they were not examined with microanalytical methods or because the authors were not aware of the possible compositional heterogeneity in single-phase polycrystalline samples [e.g., *Akimoto et al.*, 1957; *Hauptman*, 1974; *Rahman and Parry*, 1978; *Tucker*, 1981; *Moskowitz*, 1993]. Only few studies have considered the possible influence of the high-temperature nonstoichiometry of Tmt on its Curie temperature [*Hauptman*, 1974; *Rahman and Parry*, 1978; *Moskowitz*, 1987; *Wanamaker and Moskowitz*, 1994]. Since the concentration of cation vacancies at a given Tmt composition decreases both with decreasing temperature and oxygen fugacity during synthesis [e.g., *Aragon and McCallister*, 1982; *Senderov et al.*, 1993; *Aggarwal and Dieckmann*, 2002; *Lattard et al.*, 2005], these parameters should also be considered in establishing calibration curves for T_C. This point is important for the application to natural titanomagnetites. Curie temperatures derived from single-phase Tmt synthesized at 1275 to 1400°C, with unknown, but possibly high, vacancy concentrations are not directly comparable to those of titanomagnetites that crystallized in basalts at temperatures ≤1100°C with expectedly low vacancy concentrations.

[5] Another, not sufficiently understood factor to be considered for the determination of Tmt composition from T_C is the influence of the cation distribution within the Tmt structure on the magnetic properties. There is considerable disagreement in the literature upon the cation distribution in Tmt and its temperature dependence [e.g., *Akimoto*, 1954; *Néel*, 1955; *Chevallier et al.*, 1955; *O'Reilly and Banerjee*, 1965; *Stephenson*, 1969; *Bleil*, 1976; *Trestman-Matts et al.*, 1983; *Wechsler et al.*, 1984; *O'Neill and Navrotsky*, 1984] (see also review by *Waychunas* [1991]). In fact, it is obvious that the equilibrium cation distribution during high-temperature synthesis must be temperature-dependent, but the question is whether it can be frozen in during quenching and may be altered during the magnetic measurements at temperatures up to 700°C. Whereas earlier studies suggested distinct cation distributions in Tmt quenched from different temperatures [e.g., *Akimoto et al.*, 1957; *O'Reilly and Banerjee*, 1965; *Stephenson*, 1969; *Bleil*, 1971, 1976], *Wechsler et al.* [1984] found no significant difference in the unit cell parameters or magnetization determined in Tmt samples quenched from temperatures of 930 to 1350°C or annealed at 800°C. *Jensen and Shive* [1973] stated that electron diffusion in Tmt is too rapid to preserve a high-temperature equilibrium distribution by quenching but that the distribution may well depend on the ambient temperature of measurement. *O'Neill and Navrotsky* [1984] proposed that differences in samples quenched from different high temperatures may have been complicated by imperfect control of stoichiometry. In the same line of reasoning, *Wanamaker and Moskowitz* [1994] suggested that long-range ordering in an intermediate titanomagnetite (60% of the ulvöspinel end-member, i.e., ''TM60'') is a function of nonstoichiometry, with higher cation vacancies producing a more random cation distribution. They concluded that this effect may explain the differences among earlier cation distribution models.

[6] To our knowledge, an important methodological aspect has not been considered in previous studies that used T_C values retrieved from χ-T curves to estimate the composition of titanomagnetites. The majority of the T_C values used for calibration have been obtained from temperature-dependent saturation magnetization (M_s-T) curves, not from temperature-dependent susceptibility (χ-T) curves. *Deutsch et al.* [1981] have shown that for synthetic TM60 titanomagnetite, the Curie temperature obtained from M_s-T curves is close to that derived from χ-T curves and *Rahman and Parry* [1978] state that both types of values agree within ±5°C. However, we know of no further comparison between T_C values retrieved from the two types of measurements.

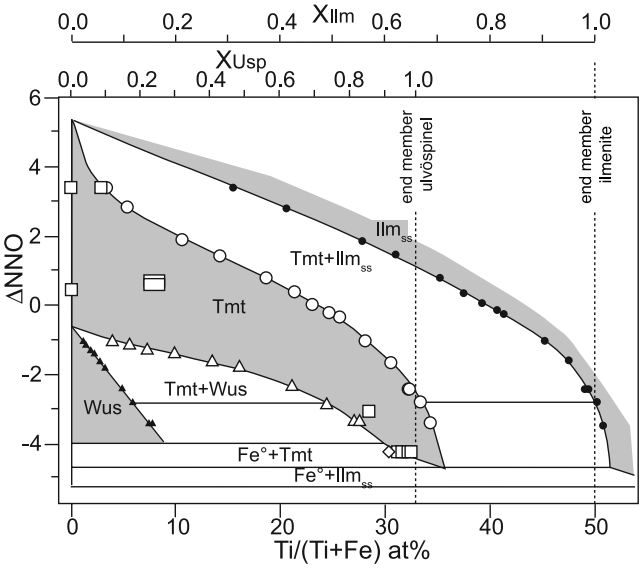

Figure 2. Phase diagram showing the chemical composition of titanomagnetites and other coexisting Fe-Ti oxide phases synthesized in the present study at 1300°C under different oxygen fugacities. The oxygen fugacities are given as ΔNNO = log fO_2 (sample) − log fO_2 (Ni-NiO buffer). Single-phase fields are gray, two-phase fields white. In the latter fields, two tie lines at the same oxygen fugacity are exemplified by thin horizontal lines. Symbols point to the phase assemblages: circles for Tmt-Ilm_{ss}; triangles for Tmt-Wus; diamond for Tmt-Fe°; squares or rectangles for single-phase Tmt (rectangles point to compositional range in case of heterogeneous Tmt). Open symbols are for Tmt; solid symbols are for Wus or Ilm_{ss}.

[7] The main goal of the present study is to improve the calibration curve for the compositional dependence of the Curie temperature of titanomagnetite on the basis of temperature-dependent magnetic susceptibility curves measured on synthetic titanomagnetites in the Fe-Ti-O system. In order to assess the possible influence of high-temperature cation vacancies onto the magnetic properties, we have synthesized two types of polycrystalline Tmt-bearing assemblages in subsolidus conditions at 1300°C (Figure 2). As known from previous experimental studies [e.g., *Taylor*, 1964; *Dieckmann*, 1982; *Aragon and McCallister*, 1982; *Senderov et al.*, 1993; *Lattard*, 1995; *Aggarwal and Dieckmann*, 2002] titanomagnetites in coexistence with ilmenite-hematite solid solution (Ilm_{ss}) are expected to have the highest possible vacancy concentrations at the temperature of interest, those in paragenesis with wüstite (Wus) should be devoid of vacancies. For comparison to previous studies, some single-phase Tmt samples (1300°C) were also considered. For more relevance to basalts, we have also examined Tmt-Ilm_{ss} assemblages synthesized at 1100°C. We have taken special care to synthesize samples in which the titanomagnetite is chemically homogeneous, both within the crystals and over the whole polycrystalline sample. In a few cases, chemical zonations or local chemical heterogeneities are present in the synthetic samples and we shall show in the following how these features influence the magnetic properties. We have also considered possible methodological artefacts by comparing T_Cs retrieved from temperature-dependent susceptibility versus saturation magnetization curves (χ-T versus M_s-T curves).

2. Methods

2.1. Syntheses

[8] All syntheses were performed at 1100 or 1300°C (subsolidus conditions) in vertical quench furnaces under a variety of oxygen fugacities fixed either by CO/CO_2 gas mixtures or by solid-state oxygen buffers (only for 1100°C synthesis). The temperature was measured before and after the runs with a type S ($Pt\text{-}Pt_{90}Rh_{10}$) thermocouple calibrated against the melting points of silver (960.8°C) and gold (1064.4°C). To ensure a complete equilibration of the synthesis products, runs lasted >24 hours at 1300°C, but up to 168 hours (7 days) at 1100°C.

[9] The starting mixtures were prepared from dried TiO_2 (99.9%, Aldrich Chemical Comp. Inc.), dried Fe_2O_3 (99.9%, Alpha Products), as well as dried and reduced (under H_2, 500°C) metallic iron (99+%, Heraeus) which were weight in stoichiometric proportions, ground together and mixed under acetone in an agate mortar and pressed to pellets of 200–300 mg (about 5 mm diameter, 4 to 6 mm in length). Metallic iron was employed only in starting mixtures for experiments performed with solid-state oxygen buffers. In this case, the original oxygen content of the sample should be close to that of the run product because of the restricted buffer capacity.

[10] For the solid-state buffer experiments, pellets of sample and buffer material (iron-wüstite, wüstite-magnetite, cobalt-cobalt oxide, fayalite-magnetite-quartz or nickel-nickel oxide) were inserted in silica-glass tubes, which were evacuated with a rotary vane pump to a vacuum in the order of 10^{-2} mbar prior to sealing. A silica-glass filler rod was used to minimize the internal volume of the ampoule and to separate the sample from the buffer. At the end of the experiments, the silica-glass ampoules were pulled out of the furnace and quenched into water, a procedure that lasted less than one minute. In all runs referred to in this paper all buffer phases were still present after termination of the experiments, i.e., the desired oxygen fugacity was maintained during the whole experiment.

[11] For the gas-mixing experiments, the sample pellets were placed on a grid of platinum wire. As sample and metal only share a very small surface and no melt ever occurs in the samples, negligible Fe loss to the wire, but maximum contact of sample with gas mixture can be achieved. High-purity CO (CO > 99.97 vol %) and CO_2 (CO_2 > 99.995 vol %) gases were mixed with electronic valves (Millipore) and allowed to flow from the bottom to the top of the furnace tube (inner diameter 4 cm) at a rate of 200 cm^3/min. The oxygen fugacity was measured after the experiments with an yttria-stabilized zirconia sensor (SIRO2) with air as the reference. The sensor was calibrated at 1300°C against the Ni-NiO equilibrium [*O'Neill and Pownceby*, 1993]. We estimate the accuracy of the experimental fO_2 values at about ±0.2 log unit at moderate to low oxygen fugacities (ΔNNO < +1; CO > 1 vol %), but up to about ±0.5 log unit at high fO_2 (more details from *Lattard et al.* [2005]). All fO_2 values given for the gas-mixing experiments in the following (Table 1) are those measured with the zirconia sensor. Since we also list the CO contents

Table 1. Synthesis Conditions and Modal Compositions of Synthetic Titanomagnetite-Bearing Samples, Chemical Compositions, and Curie Temperatures

		Synthesis Conditions						Tmt, vol %		Tmt Chemistry Ti/(Ti+Fe) (at.%)				Tc From χ-T Curves,[h] K					
														Peak Position		1/χ Method		Grommé Method	
Run	Bulk Ti/(Ti+Fe), at. %	T, °C	t, hours	Buffer[a] or CO%[b]	log fO_2[c]	ΔNNO[d]	Phases	Mean[e]	1σ[e]	Mean[f]	1σ[f]	X_{Usp}[g]	Ms-T Tc, K Heat	Heat	Cool	Heat	Cool	Heat	Cool
6F92x0	8.0	1300	25	0.0	−3.4	3.3	Tmt+Ilm	62	(2)	2.80	(10)	0.084	828	830	831	831	838[i]	838	846
6F92x0.15b	8.0	1300	22	0.2	−3.9	2.8	Tmt+Ilm	89	(3)	5.64	(8)	0.169	786	778	772	784	779	786	780
6F80x0.5a	20.0	1300	40	0.5	−4.8	1.9	Tmt+Ilm	59	(6)	10.89	(8)	0.327	690	675	689	676	693[i]	682	698
6F80x0.75b	20.0	1300	24	0.7	−5.2	1.4	Tmt+Ilm	79	(2)	14.30	(14)	0.429		586	620	590	628	594	636
6F76x0.75b	23.5	1300	24	0.7	−5.2	1.4	Tmt+Ilm	61	(6)	14.30	(14)	0.429	612	586	622	593	629	596	640
6F72x1.5	28.0	1302	24	1.5	−5.9	0.8	Tmt+Ilm	58	(3)	18.36	(13)	0.551	520	486	522	486	524	492[i]	545
6F69x1.5	31.0	1302	24	1.5	−5.9	0.8	Tmt+Ilm	23	(11)	18.36	(14)	0.551		483	524	490	524[i]	492	558[i]
6F72x2.4	28.0	1299	25	2.4	−6.4	0.3	Tmt+Ilm	79	(3)	20.92	(11)	0.628	445	415	442	419	447[i]	422	462
6F76x3.4	24.0	1299	47	3.4	−6.7	0.0	Tmt+Ilm	95		22.73	(17)	0.682	398	365	389	371	395[i]	372	402
6F72x4.4	28.0	1300	20	4.4	−7.0	−0.3	Tmt+Ilm	78	(5)	24.42	(13)	0.733	349	319	334	324	342	326	350
F72 (f) 6	27.6	1300	22	5.8	−7.1	−0.4	Tmt+Ilm	93		25.32	(18)	0.760		302	315	311[i]	325	312	328
M1300-8	31.0	1300	24	8.2	−7.7	−1.0	Tmt+Ilm	66	(6)	27.77	(17)	0.833		*235*		*237*		*238*	
6F57x18	43.3	1301	24	18.0	−8.3	−1.6	Tmt+Ilm	30	(6)	30.20	(13)	0.906		*187*		*187*		*193*	
6F63x34	37.0	1300	28	34.0	−9.1	−2.4	Tmt+Ilm	78	(3)	32.09	(10)	0.963		145	148	147	149[i]	149	150
6F57x34	43.3	1300	28	34.0	−9.1	−2.4	Tmt+Ilm	35	(6)	32.16	(9)	0.965		*147*		*148*		*152*	
6IT60x49	40.0	1300	24	49.0	−9.7	−3.0	Tmt+Ilm	45	(4)	33.60	(14)	1.008		*128*		*129*		*132*	
6F57x66	43.3	1299	18	66.0	−10.2	−3.5	Tmt+Ilm	48	(3)	34.39	(17)	1.032		109		109		114	
6F100x0	0.0	1300	25	0.0	−3.4	3.3	Tmt	100		0.00		0.000		*865*		*866*		*869*	
6F100x2.4	0.0	1300	45	2.4	−6.4	0.3	Tmt	100		0.00		0.000	851	864	873	865	879	868	880
6F97x0	3.0	1300	25	0.0	−3.4	3.3	Tmt	100		2.65	(5)	0.080		*824*	*823*	*832*	*850*[i]	*836*	*850*
6F72qx71	28.0	1299	25	71.0	−10.4	−3.1	Tmt	100		28.29	(16)	0.849		*200*		*204*[i]		*205*	
6F69x81	31.0	1300	25	81.0	−10.9	−4.2	Tmt	100		30.94	(20)	0.928		*144*		*145*		*148*	
6F69x81.5	31.0	1299	51	81.5	−10.9	−4.2	Tmt	100		31.39	(27)	0.942		*139*		*140*		*146*	
8F68x81	32.0	1300	25	81.0	−10.9	−4.2	Tmt	100		31.95	(11)	0.959		*128*		*130*		*135*	
6F67x81	33.0	1300	25	81.0	−10.9	−4.2	Tmt	100		32.95	(11)	0.989		*117*		*118*		*120*	
6F97x10	3.0	1300	26	10.0	−7.7	−1.1	Tmt+Wus	75		3.71	(5)	0.111		787	792	787[i]	792[i]	794[i]	806[i]
6F97x11	3.0	1300	28	11.0	−7.8	−1.2	Tmt+Wus	39		5.57	(8)	0.167	751	753	760	752[i]	760[i]	760[i]	768[i]
6F97x12	3.0	1300	23	12.0	−7.9	−1.3	Tmt+Wus	56	(5)	6.93	(7)	0.208		726	729	726[i]	729[i]	730[i]	736[i]
6F92x14	8.0	1300	23	14.0	−8.1	−1.5	Tmt+Wus	76		9.71	(9)	0.291	670	661	668	664[i]	671[i]	669	675[i]
6F92x18	8.0	1300	52	18.0	−8.3	−1.6	Tmt+Wus	46		13.38	(10)	0.401	595	585	596	586	595[i]	594	600[i]
6IT90x18	10.0	1300	52	18.0	−8.3	−1.6	Tmt+Wus	67		13.42	(6)	0.403	593	582	591	586	592[i]	592	597[i]
6F90x23.5	10.0	1300	22	23.5	−8.6	−1.9	Tmt+Wus	60	(5)	15.85	(12)	0.476		524	529	524	529	528	536
6F80x34	20.0	1300	20	34.0	−9.1	−2.4	Tmt+Wus	81	(5)	21.09	(15)	0.633	412	*384*	*400*	*386*	*400*	*389*	*414*[i]
6F83ax34	17.0	1300	20	34.0	−9.1	−2.4	Tmt+Wus	75	(5)	21.10	(13)	0.633		388	401	397	407	400	410
6F83ax49	17.0	1300	24	49.0	−9.7	−3.0	Tmt+Wus	62	(9)	23.69	(12)	0.711		319	329	324	332	326	340[i]
6F83x66	17.0	1300	25	66.0	−10.2	−3.5	Tmt+Wus	42	(11)	26.79	(12)	0.804		239	242	240	241	254	260
6F76x66	23.5	1300	25	66.0	−10.2	−3.5	Tmt+Wus	67	(1)	27.07	(10)	0.812		*235*		*238*[i]		*248*	
6F80x81	20.0	1300	25	81.0	−10.9	−4.2	Tmt+Fe°	81	(4)	30.17	(25)	0.905		*158*		*158*		*162*	
F76 (c) 3	23.5	1100	72	1.3	−7.7	1.2	Tmt+Ilm	52	(6)	13.87	(25)	0.416	606	593	629	593	640[i]	604	688
3F69x1.25	31.0	1101	144	1.25	−8.4	0.5	Tmt+Ilm	41	(2)	18.52	(10)	0.556		470	506[i]	474		476	558
3F69Qe	31.0	1098	120	NNO	−8.9	0.0	Tmt+Ilm	36	(1)	20.14	(15)	0.604		439	450	443	462[i]	445	468
3F76Qe	24.0	1098	93	NNO	−8.9	0.0	Tmt+Ilm	86	(3)	20.22	(19)	0.607	460	423	443	427[i]	446[i]	432	456
F63 (f) 3	37.0	1100	120	FMQ	−9.7	−0.7	Tmt+Ilm	71	(1)	23.26	(19)	0.698	368	344	352	345	373[i]	354	388
F69 (X) 3	31.0	1104	72	5.5	−9.8	−0.9	Tmt+Ilm	85	(3)	24.69	(21)	0.741		303		303		307	
F72 (X) 3	28.0	1104	72	5.5	−9.8	−0.9	Tmt+Ilm	48	(3)	24.87	(18)	0.746		*300*		*303*		*303*	
F63 (g) 3	37.0	1100	93	Co/CoO	−10.4	−1.5	Tmt+Ilm	56	(2)	26.36	(25)	0.791		*260*		*263*		*264*	
3P69WM	31.0	1100	144	WM	−11.0	−2.0	Tmt+Ilm	66	(5)	27.54	(12)	0.826		*217*		*218*		*226*	

Table 1. (continued)

Run	Bulk Ti/(Ti+Fe), at. %	Synthesis Conditions					Tmt, vol %		Tmt Chemistry				Tc From χ-T Curves, [h] K					
		T, °C	t, hours	Buffer[a] or CO%[b]	log fO_2[c]	ΔNNO[d]	Phases	Mean[e]	1σ[e]	Ti/(Ti+Fe) (at.%) Mean[f]	1σ[f]	X_{Usp}[g]	Ms-T Tc, K Heat	Peak Position Heat	Peak Position Cool	1/χ Method Heat	1/χ Method Cool	Grommé Method Heat	Grommé Method Cool
3F63x16.5	37.0	1100	135	16.5	−10.9	−2.0	Tmt+Ilm	47	(2)	28.52	(18)	0.856		*206*		*208*		*209*	
3F63x30	37.0	1100	96	30.0	−11.5	−2.6	Tmt+Ilm	82	(2)	29.81	(26)	0.894		*170*		*172*		*173*	
3P63IW	37.0	1100	144	IW	−13.3	−4.4	Tmt+Ilm	66	(2)	32.38	(14)	0.971		*122*		*122*		*123*	
3IT60IW	40.0	1100	153	IW	−13.3	−4.4	Tmt+Ilm	55	(4)	32.46	(16)	0.974		*118*		*118*		*119*	
M1100-13	43.5	1100	120	IW	−13.3	−4.4	Tmt+Ilm	36	(4)	32.95	(10)	0.989		*116*		*117*		*118*	
3F92x30	8.0	1100	177	30.0	−11.5	−2.6	Tmt+Wus	38	(3)	14.38	(12)	0.431	562	*544*	*557*	*544*	*557*[i]	*550*	*564*

[a] Abbreviations of the buffer names: FMQ, fayalite-magnetite-quartz; IW, iron-wüstite; MW, magnetite-wüstite; NNO, Ni-NiO.
[b] Volume percent of CO in the CO-CO_2 gas mixtures.
[c] The log fO_2 values derived from emf measurements with a zirconia cell or from buffer values; log fO_2 values for oxygen buffers from *O'Neill* [1987] (FMQ); *O'Neill* [1988] (IW, WM); *O'Neill and Pownceby* [1993] (NNO, Co/CoO).
[d] ΔNNO = log fO_2(experimental) − log fO_2(NNO buffer).
[e] Mean and standard deviation over three to six image analyses. If no value is given for 1σ only one image analysis was performed.
[f] Mean and standard deviation over ten single EMP analyses.
[g] $X_{Usp} = 3Ti/(Ti + Fe)$ (atomic proportion).
[h] T_c from χ-*T* curves from heating (heat) and cooling (cool) paths. T_c values obtained from χ-*T* curves measured with KLY 2 are in italic.
[i] Approximate Curie temperature estimated from complex χ-*T* curves or from those with rounded peaks (see section 5.1).

of the gas mixtures, the readers can easily retrieve the fO_2 values from the tables of *Deines et al.* [1974] for comparison. Run products were generally drop-quenched into water at the bottom of the furnace, a procedure which ensures a very fast cooling (within 10 s). In a few cases, however, the gas flow was first turned off and the samples were pulled out of the furnace and quenched into water. The whole procedure usually took less than 1 minute. In the following it is referred to as "external quench."

[12] All run products were carefully characterized using optical microscopy, X-ray powder diffraction, BSE images from a scanning electron microscope (SEM), including image analysis to determine modal proportions, and chemical analyses with the electron microprobe (EMP).

2.2. Magnetic Measurements

[13] The AC magnetic susceptibility (χ) was measured as a function of temperature in the range between 80 and 970 K on small chunks (5 to 25 mg) of the pellets retrieved from all synthesis runs. We used both a KLY 2 and a KLY 4 Kappabridge, combined with a CS-2/CS-L furnace (AGICO; see details from *Hrouda* [1994]) operating at a low field of 300 A/m and a frequency of 870 Hz for KLY 4 and 920 Hz for KLY 2. The measurements were performed in two steps. First, the samples were cooled down to 80 K with liquid nitrogen and temperatures and susceptibilities were recorded during the subsequent warming up to 273 K. In a second step, the magnetic susceptibility was measured during a heating and cooling cycle from room temperature to 970 K and back to room temperature. The heating rate was 10 K/min. To avoid mineral reactions with atmospheric oxygen, the measurements were performed in a flowing argon atmosphere (110 ml/min). The temperature was measured with a Pt resistance thermometer that was placed within 1 mm distance to the sample. According to the manufacturer of the resistance thermometer (JUMO), the recorded temperature values are accurate within ±1 K at temperatures up to 423 K but within ±3 K in the range 423–973 K. The raw susceptibility data were corrected for the empty furnace and normalized to the susceptibility magnitude at 273 K. Repeated χ-*T* measurements with the same kappabridge on different chunks of the same sample yield T_C from the heating curve that are all within ±5°, i.e., show a good reproducibility. At temperatures above room temperature, however, the T_C retrieved with kappabridge KLY 4 are up to 12 K higher than those obtained with KLY 2. The reasons for this discrepancy are not clear, but in the following we shall rely essentially on the values measured with the KLY 4 Kappabridge. Practically all T_C values above room temperature that are listed in Table 1 have been obtained with the latter apparatus (only 3 exceptions!). To avoid any confusion, the T_C values retrieved with the KLY2 are in italics in Table 1.

[14] Thermomagnetic curves were obtained using a variable field translation balance (VFTB) at the Department for Earth and Environmental Sciences at the Ludwig-Maximilian Universität, Munich. Details on the method are given by *Leonhardt* [2006]. Prior to the thermomagnetic curves, hysteresis loops at room temperature were measured with the VFTB (maximum magnetic field H = 0.63 T) in order to determine the saturation fields. M_s-*T* curves were obtained by measuring the induced magnetization from

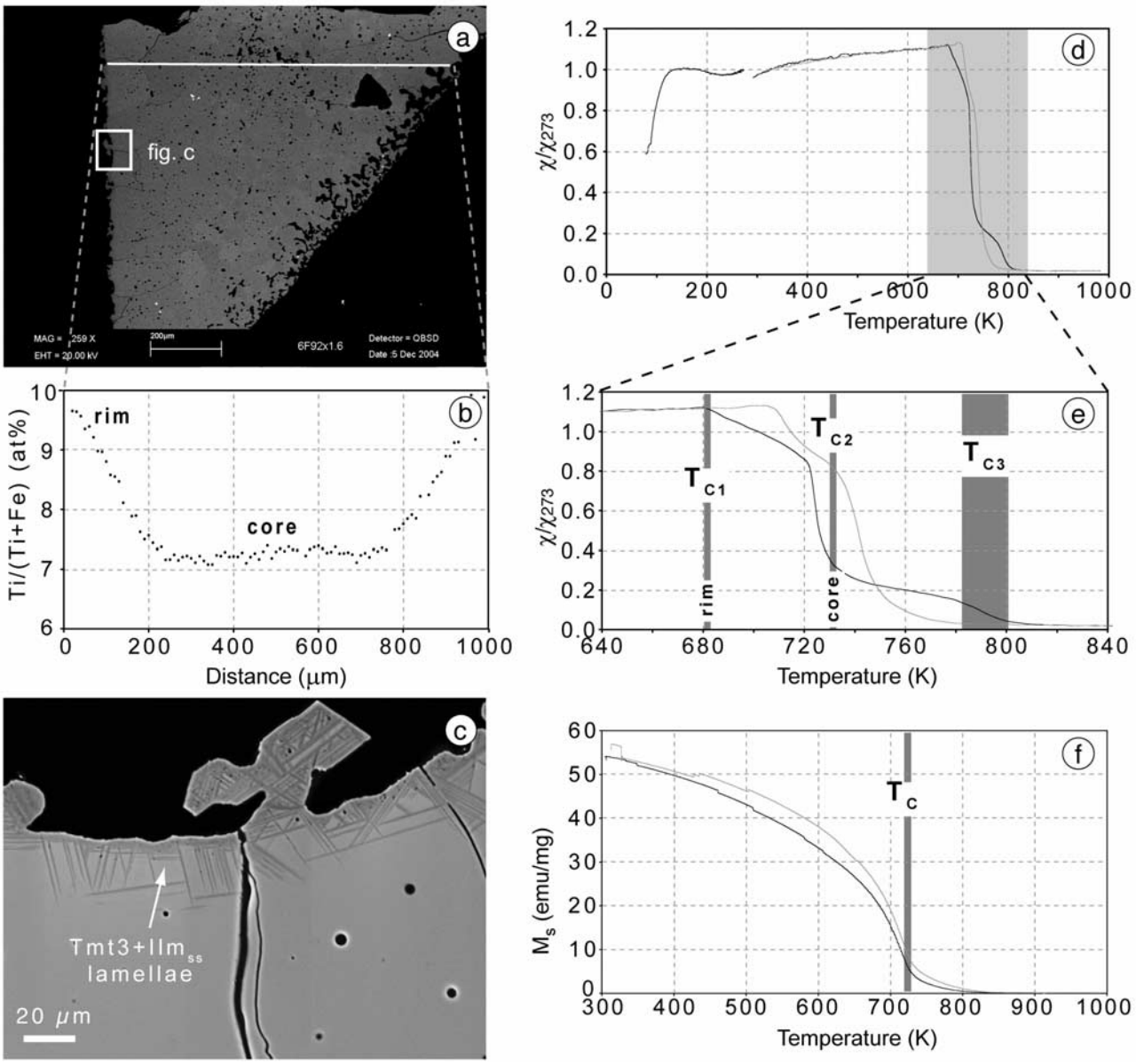

Figure 3. Effect of chemical heterogeneity on the magnetic properties of a synthetic polycrystalline titanomagnetite sample (run product 6F92x1.6; bulk X_{Usp} = 0.24; synthesized through a single sintering at 1300°C in a CO/CO_2 gas mixture). (a) BSE image of a polished section through part of the sample. (b) Ti/(Ti + Fe) values along the profile marked on Figure 3a, showing a pronounced chemical zonation with a plateau in the core region and increasing Ti/(Ti + Fe) values toward the outer surface. (c) BSE image of a small region near the surface, showing Ilm_{ss} lamellae and their Fe-rich Tmt-host crystals (Tmt3) in the outer 30 μm thick rim, resulting from oxy-exsolution during external quench (see text in sections 2.1 and 3). (d) χ-T curve in the temperature range 77–970 K (black, heating; gray, cooling). (e) Detail of the previous χ-T curve in the temperature range 640–840 K to better show the stepwise drop of the magnetic susceptibility with increasing temperature. The Curie temperatures represented by the vertical bars T_{C1} and T_{C2} have been estimated from rim and core compositions (Figure 3b), using polynom 1 in Table 3. The T_{C3} bar is deduced from approximate compositions of the near-surface, oxidized titanomagnetite (see Figure 3c). (f) M_s-T curve over the temperature range 300–970 K. Curie temperature (T_C) retrieved with the method of *Moskowitz* [1981].

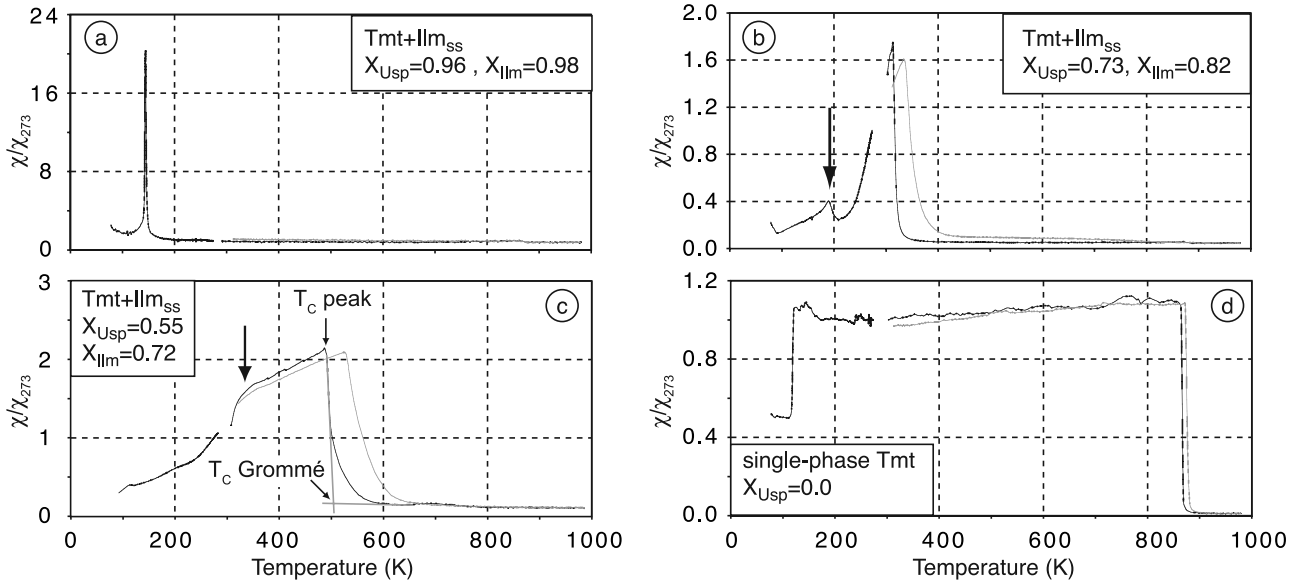

Figure 4. Examples of χ-T curves (magnetic susceptibilities normalized to the room temperature values) for titanomagnetite-bearing assemblages synthesized in the Fe-Ti-O system at 1300°C, with decreasing X_{Usp} from Figure 4a to 4d. Black curves were recorded during heating, gray curves during cooling. Note the peak or shoulder contributed by Ilm_{ss} (arrows) in Figures 4b and 4c. In Figure 4c, graphical estimates of the Curie temperature (T_C) with the intersecting tangents method of *Grommé et al.* [1969] and the peak method. Samples IDs are (a) 6F63x34, (b) 6F72x4.4, (c) 6F72x1.5, and (d) 6F100x2.4. Synthesis conditions are given in Table 1.

room temperature to 970 K in argon atmosphere at saturation fields as determined from the hysteresis loops (see description of the method by *Matzka et al.* [2003]).

3. Synthesis Products

[15] All run products consist of polycrystalline, roughly equigranular aggregates, with grain sizes around 10 to 50 μm. The majority of these run products consist of assemblages of two coexisting oxide phases, either Tmt + Ilm_{ss} or Tmt + Wus (Figure 2), which have been synthesized either at 1300°C or at 1100°C. For comparison, we have also synthesized a few titanomagnetite single-phase samples (Figure 2). The run conditions, the modal composition of the samples and the chemical composition of the synthetic titanomagnetites are given in Table 1, together with the Curie temperatures determined from temperature-dependent magnetic susceptibility curves or from temperature-dependent saturation magnetization curves.

[16] With the exception of wüstite, which unmixes tiny titanomagnetite crystals during quenching [e.g., *Simons and Woermann*, 1978; *Senderov et al.*, 1993], the drop-quenched run products show no sign of any chemical or textural changes during quenching. In all drop-quenched, two-phase run products, the relatively large titanomagnetite crystals are chemically homogeneous, within the crystals and over the whole sample [cf. also *Lattard et al.*, 2005]. Only this type of samples has been used to recalibrate the compositional dependence of the Curie temperature of titanomagnetite.

[17] However, we wish to caution against some commonly used synthesis procedures which yield samples with inhomogeneous titanomagnetite. For instance, different titanomagnetite compositions appear in products of gas mixing runs that were not drop quenched but instead were pulled out of the furnace after the turning off of the CO gas and quenched into water outside the furnace (external quench). Through this procedure the still glowing samples (T > 800°C) are exposed to air for a few seconds. The outermost rim of these samples generally displays exsolution features in form of very fine lamellae or rims of Ilm_{ss} within or around the Tmt crystals (Figure 3c), or of Psb_{ss} lamellae in Ilm_{ss} host crystals. The composition of the Tmt crystals containing Ilm_{ss}-lamellae is iron richer than those in the central part of the sample pellet. Such features may appear in single-phase samples as well as in two-phase products. In any case, they are restricted to the outermost surface of the sample or to superficial cracks, i.e., to regions of the samples that were in contact with the surrounding gas during the external quench [*Lattard et al.*, 2005]. These exsolutions can be understood as "oxy-exsolutions" in the sense of *Buddington and Lindsley* [1964]. The zones affected by oxy-exsolution represent only few percent of the total volume of the sample pellets, but (as we shall see in the following) they can significantly influence the magnetic properties of the samples. Such features were most probably present in some of the synthetic products used in other studies but have not been described because the authors did not (in older studies could not) examine their samples with the SEM.

[18] The second type of chemically inhomogeneous titanomagnetites occur in some single-phase samples that were synthesized through gas mixing experiments from starting mixtures containing only Fe_2O_3 and TiO_2 (without metallic iron). The sample pellets present outer shells (up to 200 μm thick) in which the Ti/Fe ratio increases toward the pellet surface (Figure 3b). Whether some samples used in previous magnetic studies may have presented such Ti-enriched rims is a matter of conjecture. It has been known for long that at least

Table 2. Comparison of Estimates of the Curie or Néel Temperatures Obtained With Different Graphical or Extrapolation Methods From χ-T or M_s-T Curves of a Few Standard Substances[a]

		Estimates From χ-T			Estimates From M_s-T	
Substances	Literature	Peak	$1/\chi$	Grommé	Moskowitz	Grommé
Ni (99.998%)	631	628–632	635	636	636	636
Fe_3O_4 (6F100x2.4)	848–858	864	865	868	851	852
Fe_2O_3 (99.9%)	948	950–953	951	973	952	953
Fe° (99.998%)	1043	1039–1043	1045	1052	1050	1055

[a]Temperature is given in kelvins. Literature values are from *Hunt et al.* [1995]). "Grommé" refers to the intersecting tangents method of *Grommé et al.* [1969], "Moskowitz" to the extrapolation method of *Moskowitz* [1981]. Ni, spans from a rod (Koch and Light); Fe_3O_4, single-phase polycrystalline magnetite synthesized from Fe_2O_3 powder at 1300°C, log $fO_2 = -6.4$ (run product 6F100x2.4); Fe_2O_3, powder (Alpha Products); Fe, spans from a rod (Koch and Light).

double sintering is necessary to minimize chemical heterogeneities in Tmt samples synthesized from Fe_2O_3-TiO_2 mixtures [e.g., *Bleil*, 1971] and that "it is difficult to achieve a uniform distribution of Ti in the samples" [*Kakol et al.*, 1991, p. 649]. In fact, careful examination of our double-sintered run products have in some cases revealed compositional heterogeneities. In any case, efficient checks of the compositional homogeneity of synthetic titanomagnetites are mandatory but have been reported only in a few papers [e.g., *Moskowitz*, 1987; *Kakol et al.*, 1991; *Wanamaker and Moskowitz*, 1994].

4. Magnetic Susceptibility as a Function of Temperature (χ-T Curves)

[19] The χ-T curves (Figure 4) are dominated by the contribution of titanomagnetite, with distinct shapes as a function of the ulvöspinel content (X_{Usp}). At $X_{Usp} > 0.9$ the curves are flat with only a sharp "peak" (Figure 4a), the right flank of which corresponds to the sharp decrease to paramagnetic susceptiblity at temperatures above the Curie temperature (T_C). With decreasing X_{Usp}, the asymmetry of the peak increases (Figure 4b) and at $X_{Usp} < 0.7$ the low-temperature flank becomes slightly convex and the susceptibility above room temperature increases while T_C is shifted to higher temperatures (Figure 4c). Samples with end-member magnetite display a practically constant susceptibility between the Verwey transition temperature (~120 K, transition between the cubic and the monoclinic structure) and the Curie temperature (~850 K) (Figure 4d).

[20] In samples containing Ilm_{ss} with $0.7 < X_{Ilm} < 0.85$, the contribution of the rhombohedral phase to the χ-T curves is a small peak or a shoulder on the low-temperature flank of the Tmt peak (see arrows in Figures 4b and 4c). The corresponding Curie temperatures for Ilm-Hem_{ss} are in the range of 330 to 170 K and decrease with increasing X_{Ilm}, in accordance with the results of *Ishikawa et al.* [1985]. However, precise T_C values can only be recorded from samples rich in Ilm_{ss}.

[21] The χ-T curves of samples with chemically inhomogeneous titanomagnetite do not exhibit the characteristic sharp decrease of the magnetic susceptibility at temperatures just above T_C, but instead either a stepwise drop (Figures 3d and 3e) or a gradual decay of χ in the corresponding temperature range. The χ-T curves with steplike drops are typical of sample pellets that contain only titanomagnetite (single-phase assemblage) and display large Ti-rich outer rims (Figure 3b and section 3). The χ-T curves with a gradual χ decay around T_C are registered either from Tmt single-phase samples with less pronounced Ti-rich rims or from run products with an oxidized surface due to external quench. The latter samples, which consist either of single-phase Tmt or of Tmt-Ilm_{ss} assemblages, contain few volume percent of Fe-richer titanomagnetite localized at the pellet surface (Figure 3c and section 3). In the following, however, only samples with chemically homogeneous Tmts will be considered.

[22] As can be seen from Figure 4, in many of our χ-T curves the branches above room temperature are nonreversible, i.e., the Curie temperatures are not the same on the heating and on the cooling paths. Nonreversiblity occur in nearly all samples with Tmt in the compositional range $0.1 < X_{Usp} < 0.8$, even if the Tmt are chemically homogeneous. The nonreversibility of the χ-T curves will be discussed in more detail in section 5.3.

5. Curie Temperatures Retrieved From χ-T Curves

5.1. Methods for Estimating the Curie Temperature From χ-T Curves

[23] The Curie temperature (T_C) defines the transition from ferrimagnetic to paramagnetic ordering. In previous studies, T_C determinations from χ-T curves have often been performed with the graphical "intersecting tangents method" of *Grommé et al.* [1969] where T_C is defined by the intersection point of the tangent following the sharp drop of susceptibility with the one following the neighboring base line at higher temperature [e.g., *Gonzalez et al.*, 1997; *Harrison and Putnis*, 1999a; *Kontny et al.*, 2003; *De Wall et al.*, 2004]. *Hauptman* [1974] proposed a projection of the χ drop to the zero line. However, *Petrovsky and Kapicka* [2005] have emphasized that the Curie temperature is not the temperature at which magnetic susceptibility vanishes but, instead, corresponds to a second-order phase transition with a critical point at which the magnetic susceptibility is theoretically infinite. These authors see two options for retrieving T_C from χ-T curves. If the susceptibility strongly increases just below T_C (often interpreted as Hopkinson peak), as shown in Figures 4a and 4b, the corresponding temperature can be taken as T_C ("peak method"). Otherwise, T_C can be seen as the lowest temperature at which paramagnetic behavior appears, i.e., at which the Curie-Weiss law holds: $\chi_{(T>Tc)} = C/(T - T_C)$. Consequently, in a $1/\chi$ versus T plot, T_C is the lowest temperature end of a linear pattern over a significant temperature range ("$1/\chi$ method"). *Petrovsky and Kapicka* [2005] postulate that the application of the intersecting tangent method on χ-T curves overestimates the Curie temperatures. Indeed,

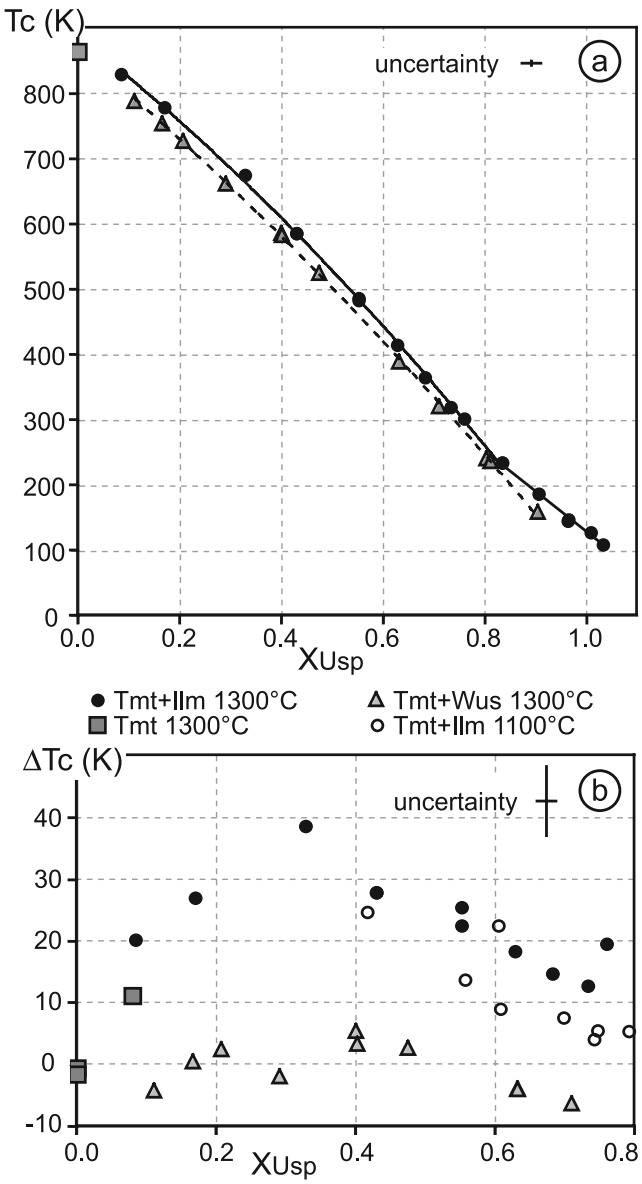

Figure 5. Curie temperatures (T_C) of synthetic titanomagnetites in the Fe-Ti-O system as a function of composition (X_{Usp}). Estimates from χ-T curves with the peak method (see section 5.1). (a) Products of syntheses at 1300°C with a second-order regression curve for Tmt in equilibrium with Wus (dashed line). For Tmt in equilibrium with Ilm_{ss}, there are two regression curves: at $X_{Usp} < 0.8$ a second-order curve (thick black curve) and at $X_{Usp} > 0.8$ a linear regression (thin black line). Equations of the regression curves are given in Table 3. (b) Plot of ΔT_C versus X_{Usp}, whereby $\Delta T_C = T_C$ (sample) $- T_C$ (regression value for Wus-bearing sample at the same X_{Usp}). The data for $X_{Usp} > 0.8$ are not represented because the extrapolation of the regression curve for Tmt (+Wus) is not adequate in this X_{Usp} range.

our χ-T measurements with the KLY 4 kappabridge on the standard substances Ni, Fe_3O_4, Fe_2O_3 and Fe° show that Curie (or Néel) temperatures are distinctly overestimated with the intersecting tangent method, whereas the peak and the $1/\chi$ methods yield values that are only a few degrees above the accepted literature values (Table 2).

[24] T_C values obtained from our samples with the different methods are listed in Table 1. We have not considered the "first derivative" approach (which identifies the peak in the first derivative of the χ-T curve) in our data set because this method yields practically the same results as the peak method. For further discussions we shall only use the values retrieved with the peak method. In case of peaks with a rounded shape, we have taken the onset of the sharp χ drop as T_C. In such cases, the $1/\chi$-T curves do not show a distinct linear portion, i.e., do not allow a good T_C estimate, because the transition from magnetically ordered to paramagnetic state does not occur at a discrete temperature, but over a (sometimes rather wide) temperature range (values followed by a superscript j in Table 1). For such samples our T_C estimate with the peak method represents the temperature at which the paramagnetic behavior starts to dominate.

[25] In samples with heterogeneous titanomagnetite compositions, which show complex χ-T curves, the determination of T_C is not straightforward. The temperature of the first significant decrease in χ appears to reflect the Ti-richest Tmt composition (Figure 3e). In case of a step-like drop at the ferrimagnetic to paramagnetic transition, further abrupt χ decreases may be correlated to some localized compositions (Figure 3), but such correlations are precarious. In case of χ-T curves with a smeared χ decrease, only the peak temperature seems to have some significance. The intersecting tangents method may yield different T_C values, but their significance is dubious.

[26] The results listed in Table 1 concern samples with chemically homogeneous Tmts, which produce simple χ-T curves. The curves for Tmt in equilibrium with Wus, however, display step-like features, due to the fact that Wus exsolves Fe-rich Tmt upon quenching (see section 3). With the peak method the T_C of the high-temperature Tmt is easily retrieved, but the $1/\chi$ and the intersecting tangents methods yield uncertain results (values followed by a superscript j in Table 1).

5.2. Curie Temperatures as a Function of Tmt Composition, Synthesis Temperature, and Paragenesis

[27] In this section we address only the Curie temperatures that can be determined from the first heating branch of the χ-T curves. As mentioned in section 4, the subsequent cooling branch generally points to different T_C values. This nonreversibility will be discussed in section 5.3.

[28] As known from previous studies (see Figure 1), the Curie temperatures of our synthetic titanomagnetites decrease with increasing ulvöspinel content (Figure 5a). Yet our data reveal a number of further interesting effects. For samples synthesized at 1300°C the T_C values for Tmt in coexistence with Ilm_{ss} are all higher than those of Tmt in coexistence with Wus (Figure 5a). This ΔT_C is in the order of 15 to 35 K (Figure 5b). At $X_{Usp} = 0.33$ ΔT_C culminates at 37 K and apparently decreases with increasing X_{Usp} up to about 0.8. At high Ti contents ($X_{Usp} > 0.9$), the comparison is difficult because Tmt can no longer coexist with wüstite in the Fe-Ti-O system (see Figure 2). Yet the trend persists for these Ti-rich compositions: Tmt synthesized in equilibrium with Ilm_{ss} do have higher T_C than single-phase Tmt with the same Ti/Fe ratio. The T_C values retrieved from Tmt-Ilm_{ss} assemblages synthesized at 1100°C are, at any given

Table 3. Coefficients and Correlation Coefficients of the Regression Polynoms Obtained for the Correlations Between Curie Temperature and Composition of Synthetic Titanomagnetites in the Fe-Ti-O System[a]

Polynom	Synthetic T, K	Compositional Range	Coexisting Oxide	a	b	c	u	v	w	R^2
1	1573	0.1 < Xusp < 0.8	Ilm_{SS}	−218.195	−608.713	887.008	−4E-7	−0.000794	1.033357	0.999
2	1573	0.8 < Xusp < 1.0	Ilm_{SS}		−628.406	755.979		−0.001579	1.201158	0.993
3	1573	0.1 < Xusp < 0.9	Wus	−154.449	−650.283	865.549	−3E-7	−0.000953	1.053392	0.999
4	1373	0.4 < Xusp < 0.8	Ilm_{SS}	−222.712	−629.299	892.454	−3E-7	−0.000856	1.029115	0.999
5	1373	0.8 < Xusp < 1.0	Ilm_{SS}		−662.873	766.905		−0.001494	1.154673	0.990
6	1573	0.1 < Xusp < 0.8	Ilm_{SS}	−400.062	−414.955	866.621	−1E-6	−0.000204	0.915024	0.999

[a]Polynoms 1 to 5 are based on T_C values retrieved from χ-T curves, polynom 6 is based on T_C values retrieved from M_s-T curves. All temperatures are in kelvins. Polynoms of the form $T_C = aX_{Usp}^2 + bX_{Usp} + c$ and $X_{Usp} = uT_C^2 + vT_C + w$. Read −4E−7 as -4×10^{-7}.

X_{Usp}, intermediate between those of the two 1300°C series (Figure 5b). For each data group one can establish a second-order polynomial correlation (with excellent correlation coefficients) between the T_C value and the ulvöspinel content of the titanomagnetites in the range $0.1 < X_{Usp} < 0.8$ (Table 3). At higher Ti contents, the slope of the regression line for Tmt in equilibrium with Ilm_{ss} is distinctly flatter (Figure 5a).

[29] The most possible explanation for the differences between the Curie temperatures of titanomagnetites synthesized in equilibrium with different phases (Ilm_{ss} versus Wus), is to assume that the two sets of Tmt have different concentrations of cation vacancies. Tmt synthesized in equilibrium with wüstite should be devoid of cation vacancies and may even contain cation interstitials. In contrast, Tmt in equilibrium with Ilm_{ss} are known to present significant concentrations of cation vacancies at 1300°C, but somewhat lower concentrations at 1100°C [e.g., *Aragon and McCallister*, 1982; *Senderov et al.*, 1993; *Aggarwal and Dieckmann*, 2002].

[30] In principal, our results confirm those of *Hauptman* [1974] and *Rahman and Parry* [1978], who reported a strong increase of the Curie temperatures (of up to 60 K) with increasing vacancy concentrations for two single titanomagnetite compositions (X_{Usp} = 0.6 and 0.3) equilibrated at 1275 or 1300°C. Yet our results show somewhat smaller T_C increases (Figure 5). This discrepancy is most probably related to the fact that *Hauptman* [1974] and *Rahman and Parry* [1978] oversaw small amounts of Ilm_{ss} in their allegedly single-phase titanomagnetite samples. According to the results of *Lattard et al.* [2005], the four highest oxygen fugacities reported by *Hauptman* [1974] for the equilibration of a Tmt with X_{Usp} = 0.6 at 1275°C are outside the stability field of single-phase Tmt but instead fall in the binary Tmt-Ilm_{ss} field (see Figure 2). Consequently, the corresponding samples of *Hauptman* [1974] probably contained some percent of Ilm_{ss} and the coexisting Tmt had a lower X_{Usp} and hence a higher T_C than expected. Some of the χ-T curves presented by *Hauptman* [1974] give support to our hypothesis. They have a step-like form (curves 5 and 6 in Hauptman's Figure 6) which suggest juxtaposed compositions of titanomagnetite. Concerning the data of *Rahman and Parry* [1978], the highest fO_2 presented for Tmt with X_{Usp} = 0.3 also falls in the binary Tmt-Ilm_{ss} field delineated at 1300°C by *Lattard et al.* [2005]. Moreover, *Rahman and Parry* [1978, p. 233] report that their thermomagnetic curves "in some cases suggest the occurrence of a higher Curie point transition" whereby the "maximum amount of this higher Curie point component . . .was about 5% by volume."

[31] In conclusion, our data set definitely shows a range of Curie temperatures for titanomagnetites with the same Ti/Fe ratio, whereby the lowest T_C is registered for Tmt coexisting with Wus, i.e., the Tmt with the lowest possible vacancy concentration, and the highest T_C for Tmt coexisting with Ilm_{ss}, i.e., those with the highest possible vacancy concentration.

5.3. Nonreversibility of the χ-T Curves

5.3.1. Experimental Results

[32] Nearly all titanomagnetites with T_C values above room temperature present χ-T curves with a conspicuous nonreversibility of the Curie temperature. In most samples the strong change in magnetic susceptiblity marking the Curie temperature is shifted to higher temperature in the χ-T pattern recorded on the cooling path compared to that of the preceding heating path (Figure 4).

[33] The difference (ΔT_C) between the two Curie temperatures obtained from the cooling and from the heating branch, respectively, is dependent not only upon the Tmt composition, but also upon the synthesis temperature and the coexisting oxide phase. Tmts coexisting with Wus have

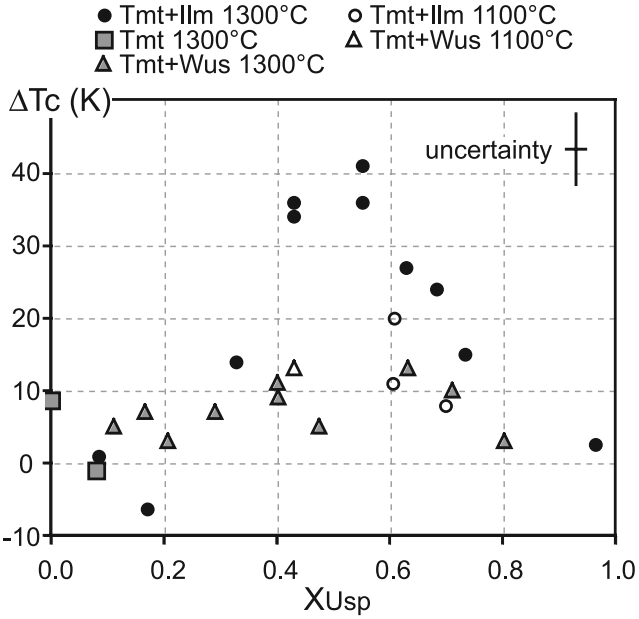

Figure 6. Difference (ΔT_C) between Curie temperatures obtained from the cooling and from the heating branch of χ-T curves as a function of titanomagnetite composition (X_{Usp}).

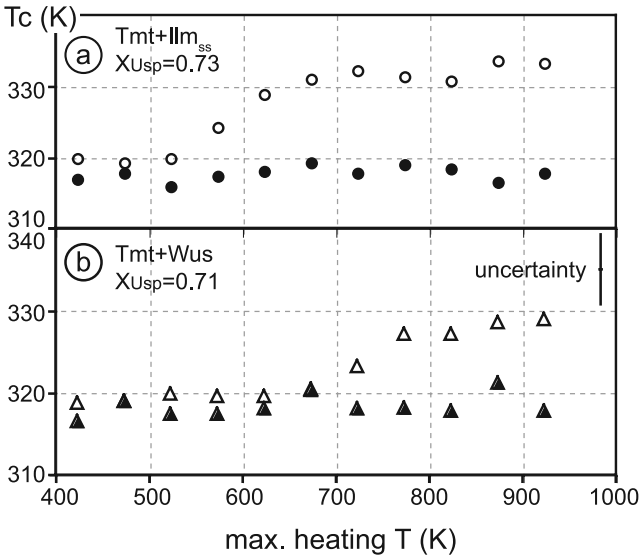

Figure 7. Curie temperatures of titanomagnetites with $X_{Usp} \approx 0.7$, retrieved with the peak method from the heating (solid symbols) and from the cooling branches (open symbols) of χ-T curves as a function of the maximum heating temperature during the χ-T measurements. (a) Tmt synthesized at 1300°C in equilibrium with Ilm_{ss} (sample 6F72x4.4). (b) Tmt synthesized at 1300°C in equilibrium with Wus (sample 6F83ax49).

the lowest ΔT_C, with nearly reversible χ-T curves for Fe-rich compositions, but a slight nonreversiblity ($\Delta T_C < 15$ K) for compositions in the X_{Usp} range 0.4 to 0.8 (Figure 6). Tmts in equilibrium with Ilm_{ss} at 1300°C present the strongest nonreversibility, which culminates at $X_{Usp} \approx 0.5$, with ΔT_C up to 40 K. For one Fe-rich composition (X_{Usp} = 0.169), however, the T_C value on the cooling branch is lower than that on the heating branch ($\Delta T_C = -6$ K). Tmts synthesized in equilibrium with Ilm_{ss} at 1100°C have much lower ΔT_C than those synthesized at 1300°C (Figure 6).

[34] Further tests show that the nonreversiblity is also influenced by the maximum heating temperature during the χ-T measurements. For example, in case of a Tmt with X_{Usp} = 0.7 synthesized at 1300°C in equilibrium with Ilm_{ss}, the χ-T curve is reversible if the maximum heating temperature does not exceed 500 K. The nonreversibility increases with increasing maximum heating temperature and reaches a plateau value for maximum heating temperatures above 700 K (Figure 7a). In case of a Tmt with practically the same X_{Usp}, but synthesized in equilibrium with Wus, nonreversibility appears only if the heating temperature exceeded 700 K (Figure 7b). Repeated heating-cooling cycles from room temperature to 970 K lead to converging heating and cooling branches, i.e., the nonreversibility disappears and the Curie temperature stabilizes at a value near that of the original T_C on the cooling branch (Figure 8).

[35] The nonreversible behavior of the χ-T curves may be related to changes in the chemical composition, either related to oxidation or to unmixing of Tmt, or in the degree of cation order of titanomagnetite. We shall examine these possibilities in sections 5.3.2–5.3.4.

5.3.2. Is the Nonreversibility due to Oxidation?

[36] The increase of the Curie temperature on the cooling branch could point to oxidation during the χ-T measurements yielding either titanomaghemite or a Fe-richer Tmt with concomitant formation of Ilm_{ss} lamellae (oxy-exsolution). In our samples, the formation of titanomaghemite can be ruled out because this phase is known to develop only from very fine grained Tmt (typically ball milled) oxidized in air at temperatures below 573 K and to quickly breakdown at higher temperatures [e.g., *Moskowitz*, 1981]. In contrast, our χ-T measurements have been performed on relatively coarse-grained assemblages under flowing Ar atmosphere and the curves were reversible when the maximum heating temperature did not exceed 573 K (Figure 7).

[37] Systematic SEM examination of all samples measured under flowing Ar have shown no typical oxy-exsolution "trellis" texture, with very fine lamellae of Ilm_{ss} in the {111} planes of magnetite-rich Tmt [e.g., *Buddington and Lindsley*, 1964; *Haggerty*, 1991]. EMP analyses have also revealed no change in the chemical composition of the Tmts before and after the χ-T measurements. The only exception was a sample, which was measured three times, i.e., with three consecutive heating-cooling cycles from room temperature to 970 K (χ-T curves in Figure 8). After the third cycle, the sample presented oxy-exsolution trellis textures in the near-surface region (rim of about 30 to 40 μm in depth).

[38] In contrast, single χ-T measurements performed in air do cause near-surface oxidation, resulting in trellis textures in the outer rim of the sample. This has been observed on one Tmt-Ilm_{ss} sample (X_{Usp} = 0.73, X_{Ilm} = 0.82). The cooling branch of the corresponding χ-T curve is distinctly different from those retrieved from our usual measurements in flowing Ar. Not only is the χ drop shifted to higher temperatures, but the curve also presents a long flat tail ending at temperatures around 840 K, which points to small amounts of magnetite-rich Tmt. Indeed, oxidation of such a Fe-Ti oxide assemblage at temperatures below 900 K should produce Fe-rich Tmt [e.g., *Buddington and Lindsley*, 1964].

[39] To summarize, we have no indication for oxidation of our samples during single χ-T measurements under Ar flow.

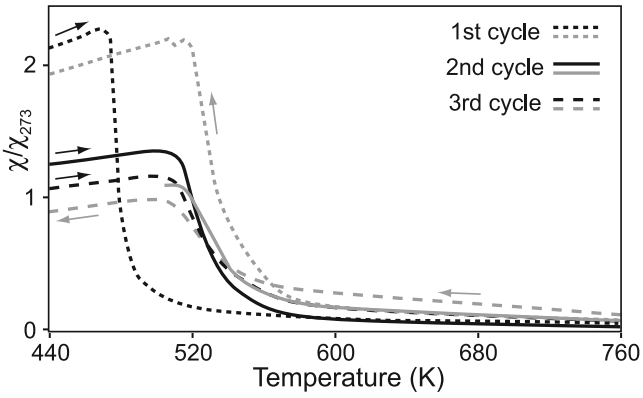

Figure 8. The χ-T curves recorded during three succeeding heating-cooling cycles (maximum heating temperature 970 K) from the same sample piece (Tmt + Ilm_{ss}, X_{Usp} = 0.55; Sample 6F69x1.5). Black curves are for heating; gray curves are for cooling.

5.3.3. Is the Nonreversibility due to Subsolvus Unmixing of Titanomagnetite?

[40] In principal, the nonreversibility of the χ-T curves could also be related to unmixing of the original high-temperature Tmts into intergrowths of a Fe-rich and a Fe-poorer spinel, caused by subsolvus exsolution during the χ-T measurements. *Harrison and Putnis* [1996] have documented such processes in the magnetite-spinel solid solution. The situation for titanomagnetite is, however, somewhat different, because the consolute point of the miscibility gap probably lies below 870 K or even 770 K [*Vincent et al.*, 1957; *Lindsley*, 1981; *Price*, 1981; *Lindsley*, 1991], i.e., at lower temperatures than the maximum heating temperature during our χ-T measurements (970 K). Therefore unmixing of Tmt during these measurements appears unlikely.

[41] In any case, the observed nonreversiblity of single-phase end-member magnetite (Fe_3O_4) cannot be related to unmixing (Run product 6F100x2.4 in Table 1 and Figures 4 and 6). In a Fe-rich Tmt, for instance with $X_{Usp} = 0.169$, unmixing would be expected to produce partial exsolution of small amounts of a Ti-richer Tmt, whereas the composition of the host Tmt would become somewhat Fe-richer. Consequently, the cooling branch of the χ-T curve should be shifted toward higher temperatures, but the contrary happens (see Figure 6). For Ti-rich titanomagnetites, unmixing would be expected to produce partial exsolution of small amounts of a Fe-richer Tmt, whereas the composition of the host Tmt would become slightly Ti-richer. Consequently, we would expect cooling branches of the χ-T curves with steps or gradual decays, such as those depicted in Figure 3 for inhomogeneous Tmts. However, such features do not occur in case of the samples listed in Table 1 (see Figure 4). The cooling branches of the χ-T curves may be somewhat smoother around T_C (Figures 4b, 4c, and 8), but otherwise they closely resemble the heating branches and do not show indication for the appearance of different Tmt compositions during the χ-T measurements.

[42] Very fine grained Tmt exsolution lamellae could be expected to have single domain behavior and display a pronounced Hopkinson peak on the cooling branch of the χ-T curve [e.g., *Harrison and Putnis*, 1996, Figure1b], but no such peak appeared in the cooling branches of our χ-T curves. In total, we do not see any indication for subsolvus unmixing of Tmt during the χ-T measurements.

5.3.4. Cation Distribution and Nonconvergent Ordering

[43] Since changes in Tmt compositions, in relation to oxidation or unmixing, do not appear to be responsible for the nonreversibility of the χ-T curves, only changes in nonconvergent cation order can be further considered. We present here first a brief outline of the theory about temperature-dependent cation distribution in titanomagnetite and the kinetics of cation reordering.

[44] The stoichiometric end-members of the titanomagnetite solid solution, magnetite and ulvöspinel, are known to have the inverse spinel cation distribution at room temperature. Their structural formula can be written as $(Fe^{3+})^{tet}$ $[Fe^{3+}\ Fe^{2+}]^{oct}\ O_4$ for the magnetite end-member and $(Fe^{2+})^{tet}$ $[Fe^{2+}\ Ti^{4+}]^{oct}\ O_4$ for the ulvöspinel end-member. At elevated temperatures, ulvöspinel is known to keep its inverse configuration [e.g., *Wechsler et al.*, 1984], whereas in magnetite cations become progressively disordered over both tetrahedral and octahedral sites (nonconvergent disordering) with increasing temperature [e.g., *Wu and Mason*, 1981; *Wiβmann et al.*, 1998]. The structural formula for a high-temperature magnetite with a random cation distribution is $(Fe^{3+}_{0.67}\ Fe^{2+}_{0.33})^{tet}$ $[Fe^{3+}_{1.33}\ Fe^{2+}_{0.67}]^{oct}O_4$.

[45] On the basis of thermoelectric coefficient measurements and of the thermodynamic study of *O'Neill and Navrotsky* [1984], *Trestman-Matts et al.* [1983] have developed a cation distribution model for the titanomagnetite solid solution as a function of equilibration temperature. Titanium is assumed to occupy only octahedral sites, in accordance with magnetic and neutron diffraction data [e.g., *O'Reilly and Banerjee*, 1965; *Stephenson*, 1969; *Ishikawa et al.*, 1971; *Wechsler et al.*, 1984]. Calculations with the model of *Trestman-Matts et al.* [1983] show, as expected, that in all Tmt at equilibrium nonconvergent disordering progresses with increasing temperature, i.e., the Fe^{2+} content in octahedral sites decreases and the one in tetrahedral sites increases (Figure 9a). On the basis of the model of *Stephenson* [1972] these changes translate into a decrease of T_C with increasing equilibrium temperature (Figure 9b). For a Tmt with $X_{Usp} = 0.7$, for example, the Curie temperature is predicted to be 342 K if the cation distribution equilibrated at 1573 K, but 371 K if the cation distribution could equilibrate at 293 K (Figure 9b). With decreasing X_{Usp} down to 0.4, the effect of the equilibrium temperature on the cation distribution become stronger, hence the differences in T_C steadily increase. At $X_{Usp} < 0.4$, however, the trend reverses (Figure 9c).

[46] Yet the kinetics of cation ordering in Tmt plays a dominant role in the interpretation of our results. On the basis of the observation that unit cell parameters and/or magnetic properties of synthetic Tmts quenched from different temperatures are identical [e.g., *O'Donovan and O'Reilly*, 1980; *Wechsler et al.*, 1984], the cation distribution established in titanomagnetite at high synthesis temperatures is reputed unquenchable. Indeed, since reequilibration requires only the transfer of an electron between Fe cations in adjacent tetrahedral and octahedral sites, its kinetics must be very rapid [*Jensen and Shive*, 1973]. However, as discussed in detail by *Harrison and Putnis* [1999b], not only the quench temperature but also the quench rate determines the quenched-in degree of order. For quench rates usual in experimental studies, *Harrison and Putnis* [1999b] suggest for Tmt that the closure temperature, i.e., the quench temperature above which the quenched-in degree of order remains constant, is less than 873 K. The quenched-in degree of order should correspond to an equilibrium order at still lower temperature, in the order of 750 to 800 K [see *Harrison and Putnis*, 1999b, Figure 16]. This would hold for all our synthetic samples.

[47] During the χ-T measurements, which involve heating and cooling up to 970 K at a rate of 10 K/min, rapid changes in cation ordering may appear above a characteristic relaxation temperature and the ordering state may even reach its equilibrium value, which will be metastably kept on cooling to room temperature [cf. *Harrison and Putnis*, 1996]. Whether such changes in cation ordering lead to a shift of the Curie temperature on the cooling branch of the χ-T curve or not, depends on the relative position of the Curie temperature and the relaxation temperature.

[48] Let us first consider a titanomagnetite synthesized in equilibrium with Ilm_{ss} with $X_{Usp} = 0.7$ and a nonreversible T_C ($\Delta T_C \approx 20$ K). The χ-T measurements performed with different maximum heating temperatures suggest a relaxation temperature of about 600 K (Figure 7a). During the first heating of a χ-T measurement, the T_C value registered at 354 K (value interpolated from our experimental data; see polynom 1 in Table 3), i.e., well below the relaxation temperature, must represent the quenched-in degree of order. Upon heating and subsequent cooling above the relaxation temperature at a rate of 10 K/min, the cation distribution might reach the equilibrium values depicted in Figure 9a. The higher T_C value recorded during cooling (about 374 K) probably reflects the equilibrium degree of order established at the relaxation temperature (about 600 K) and preserved during further cooling. The model of *Stephenson* [1972] predicts a higher T_C value on the cooling branch (Figures 9b and 9c), but the difference is much lower than the nonreversiblity observed in our χ-T measurements (only 3 to 4 K compared to the observed 20 K; Figures 9c and 6). *Harrison and Putnis* [1999b] have also noted that Stephenson's model strongly underestimates the nonreversiblity. Yet this model is useful to explain the increase in nonreversibility with decreasing X_{Usp} down to 0.4. As shown in Figure 9c, the differences between the T_C values corresponding to the equilibrium order at about 600 K (relaxation temperature) and those corresponding to the degree of order at about 750–800 K (i.e., quenched-in orders from syntheses) significantly increase with decreasing ulvöspinel content, at least down to $X_{Usp} = 0.4$ (Figure 9c).

[49] For Tmts with $X_{Usp} \leq 0.4$ the situation changes because the Curie temperature is higher than the relaxation temperature during the χ-T measurements (Figure 9c). Above the relaxation temperature, the measured T_C values mirror the equilibrium degree of order and the χ-T curves are more or less reversible. A particular case is represented by a sample with $X_{Usp} = 0.2$, which shows a lower *Tc* value on the cooling than on the heating path (Figure 6). Such a behavior has been reported by *Harrison and Putnis* [1999b] (see their Figure 19) for a spinel with the same mole fraction of the magnetite end-member in the Fe_3O_4–$MgAl_2O_4$ solid solution. Their interpretation is that for this composition T_C falls within the temperature range of the ordering hysteresis.

[50] As shown in Figure 6, Tmts synthesized in equilibrium with Wus over the whole compositional range have χ-T curves with only slight nonreversibility. This conspicuous difference to the behavior of Tmts coexisting with Ilm_{ss} is most probably related to the different vacancy concentrations in the two series of Tmt. As already discussed in section 5.2, Tmts coexisting with Wus must have the lowest vacancy concentration for any given Ti/Fe ratio and T-fO_2 synthesis conditions. Consequently they are expected to only reluctantly change their cation distribution during the χ-T measurements. Indeed, the relaxation temperature for a Tmt with $X_{Usp} = 0.73$ synthesized in equilibrium with Wus appears to be about 200 K higher

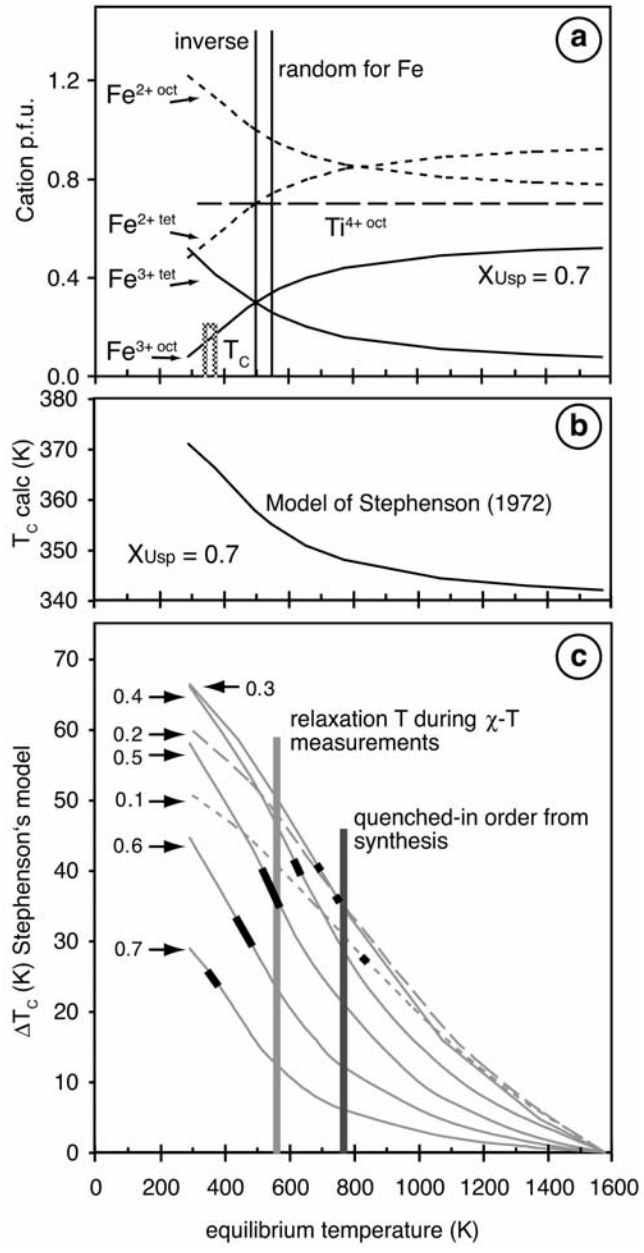

Figure 9. Relationships between Curie temperature and modeled cation distributions in Tmt. (a) Temperature-dependent cation distribution at equilibrium for $X_{Usp} = 0.7$ calculated with the model of *Trestman-Matts et al.* [1983]. Thin vertical bars mark the temperatures at which perfect inverse and random distributions are predicted; short vertical bars mark the Curie temperatures extracted from the heating and cooling branches of the χ-T curves. (b) Curie temperatures calculated with the model of *Stephenson* [1972] for the equilibrium cation distributions depicted in Figure 9a. (c) Differences (ΔT_C) between the calculated T_C values for cation distributions at equilibrium at 1573 K (1300°C) and those for equilibrium at lower temperatures for various Tmt compositions. For $0.7 > X_{Usp} > 0.3$, ΔT_C continuously increases with decreasing X_{Usp} (solid curves). At lower X_{Usp} the trend reverses (dashed curves). The black bar represents the equilibrium temperature corresponding to the quenched-in cation degree of order after synthesis at 1573 K, the gray bar represents the approximate relaxation temperature during the χ-T measurements. The thick parts on the curves are the ranges of T_C values recorded from the heating and cooling branches of the χ-T curves.

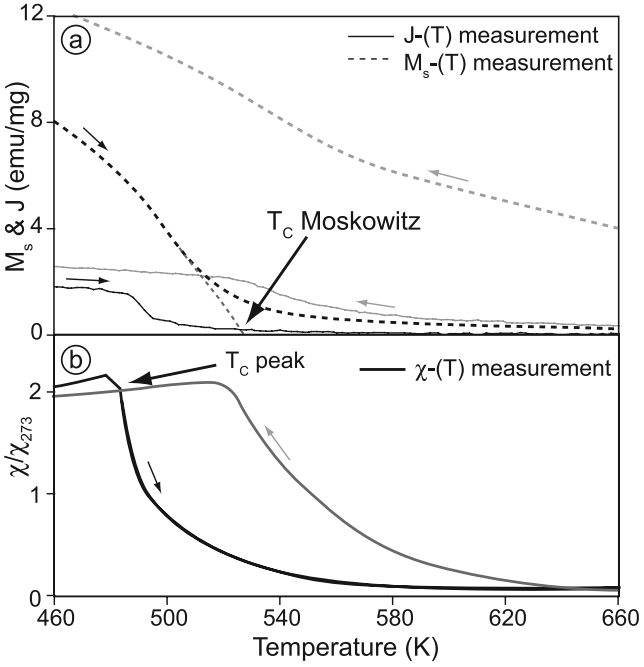

Figure 10. Comparison of temperature-dependent magnetic susceptibility (χ-T) and magnetization curves (M_s-T and J-T) measured on two chunks of the same titanomagnetite sample (Tmt + Ilm_{ss}; sample 6F72x1.5). M_s-T curve measured with a field of 5060 Oe (0.63 T), J-T curve with a field of 40 Oe, χ-T curve with 3.8 Oe. Black curves for the heating branches; gray curves for cooling branches.

than that for a Tmt with the same X_{Usp} synthesized in equilibrium with Ilm_{ss} (Figures 7a and 7b).

[51] On the same line of reasoning, the smaller nonreversiblity of Tmt synthesized in equilibrium with Ilm_{ss} at 1100°C (compared with 1300°C; Figure 6) can be related to the inverse correlation between vacancy concentration and synthesis temperature [*Aggarwal and Dieckmann*, 2002].

6. Curie Temperatures Retrieved From M_s-T Curves

[52] Since the majority of the literature data on the compositional dependence of T_C of titanomagnetite have been obtained from temperature-dependent saturation magnetization (M_s-T) curves, we have also measured, for comparison, the thermomagnetic curves of several of our Tmt-bearing synthetic samples.

6.1. Methods for Estimating the Curie Temperature From M_s-T Curves

[53] Theoretically, T_C is the temperature at which the spontaneous magnetic alignment vanishes and paramagnetic behavior dominates. In practice, T_C has often been estimated with the graphical "intersecting tangents method" of *Grommé et al.* [1969]. *Moskowitz* [1981] has shown that this method yields too high T_C values in case of complex, irregular M_s-T curves and has proposed to extrapolate the curves in the temperature range from T_C-100 to T_C with a square root function. Although our samples generally exhibit regular, continuous M_s-T curves, we have used the latter method in the version implemented by *Leonhardt* [2006]. The corresponding T_C values are listed in Table 1. Measurements on the standard substances Ni, Fe_2O_3 and Fe yield T_C values a few degrees above the accepted literature values [cf. *Hunt et al.*, 1995]; those on a synthetic Fe_3O_4 are within the range of literature values (Table 2).

6.2. Nonreversibility of the M_s-T Curves

[54] Just like the χ-T curves, most M_s-T curves are nonreversible, because their cooling branch is shifted to higher temperatures compared to their heating branch. For pure magnetite the M_s-T curve is reversible, but with increasing X_{Usp} the shift continuously increases (Table 1). In contrast to the χ-T curves, the cooling and heating branches of the strongly nonreversible M_s-T curves are not parallel. Instead, the cooling branches present flat "tails" toward high temperatures (Figure 10) and all cut the zero line at T between 800 and 850 K. The latter feature points to a small amount of magnetite-rich Tmt, which results from partial oxidation at the surface of the samples during the M_s-T measurements. Indeed, BSE images of all samples after the M_s-T measurements reveal trellis oxy-exsolution textures in the near-surface regions, whereas no sign of oxidation is recognizable on the samples prior to the M_s-T measurements. If the maximum heating temperature during the measurements did not exceed 770 K, no oxy-exsolution could be detected and the cooling branch of the M_s-T did not show any high-temperature tail. Apparently, oxidation becomes effective only at temperatures above about 800 K and is thus discernible only on the cooling branch of the M_s-T curves. One may wonder why surface oxidation occurred although the measurements were performed in Ar atmosphere. Apparently, the glass wool placed around the sample to keep it in place within the VFTB hinders the flow of Ar.

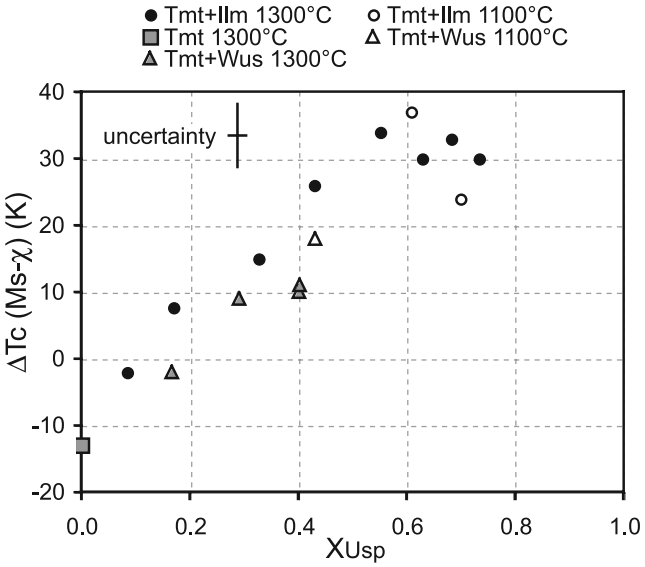

Figure 11. Difference between the Curie temperatures estimated from M_s-T and χ-T curves as a function of titanomagnetite composition (X_{Usp}).

6.3. Comparison With the T_C Values Retrieved From χ-T Curves

[55] The T_C values obtained from the heating branches of the M_s-T curves are listed in Table 1. Most of them are higher than those obtained from the heating branch of the χ-T curves, whereby the difference $\Delta T_C = T_C(M_s) - T_C(\chi)$ regularly and strongly increases (up to nearly 40 K) with increasing Ti content of the Tmt, at least up to $X_{Usp} = 0.6$ (Figure 11). At higher Ti contents no comparison is possible because the VFTB does not allow measurements below room temperature. In contrast to the ΔT_C calculated from the nonreversible χ-T curves (Figure 6), the present ΔT_C (Figure 11) does not so strongly vary with the synthesis temperature or with the synthetic assemblage (+Ilm_{ss} or +Wus). This suggests that this ΔT_C is not significantly influenced by the concentration of cation vacancies.

[56] The large ΔT_C values cannot be explained by differences in the temperature records in the two apparatuses. Measurements on standard substances yielded similar T_C values with the χ-T and the M_s-T methods with a maximum ΔT_C around 10 K, but no systematic change with temperature (see Table 2).

[57] A direct comparison of the M_s-T and χ-T curves for a sample with a Tmt of intermediate composition, together with a thermomagnetic curve (J-T) measured with a relatively low field intensity (40 Oe, instead of H = 5060 Oe, i.e., 0.63 T, for saturation) makes clear why these curves yield so different T_C values (Figure 10). In the χ-T curve, the initiation of the sharp, linear drop in susceptibility (see arrow in Figure 10b) is taken to define the Curie temperature. A similar linear drop occurs in the J-T curve and could be considered to point to the same T_C value. The concave tails of both curves at higher temperatures are not taken into account for the T_C determination. In contrast, the heating branch of the M_s-T curve gradually changes from a convex to a concave form with increasing temperature and the extrapolation to the $M_s = 0$ value [after *Moskowitz*, 1981] includes part of the concave tail or the curve, yielding a higher T_C value. Yet it is not clear what the concave tails of the heating branches of the M_s-T curves represent. As discussed in section 6.2., they do not appear to reflect oxidized portions of the samples.

[58] At present, we can only keep in mind that the temperature-dependent measurements of the saturation magnetization and of the magnetic susceptibility yield different T_C values for titanomagnetite, with increasing divergence with increasing titanium content up to X_{Usp} values of about 0.7. This discrepancy might be related to the vastly different field intensities applied for the M_s-T versus the J-T and χ-T measurements (high DC field for M_s-T measurements, low AC field for χ-T measurements), which might influence cation reordering.

7. Comparison With Literature Data

[59] As shown in Figure 5, our results constrain a much narrower range of Curie temperatures at any given X_{Usp} than the literature data compiled in Figure 1. Part of the scattering in the literature data is most probably related to chemical inhomogeneities in the titanomagnetite samples, in particular due to surface oxidation during quenching or to the formation of Ti-richer outer zones during gas mixture

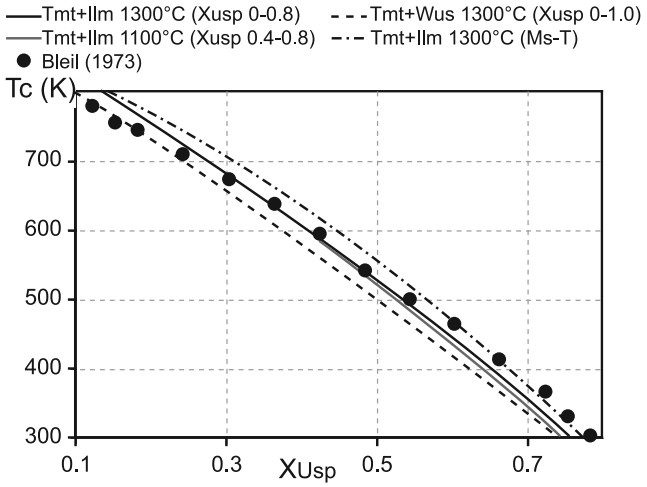

Figure 12. Compositional dependence of the Curie temperature of synthetic titanomagnetites in the Fe-Ti-O system. Comparison of the regression curves obtained from samples synthesized at 1300°C or 1100°C in the present study with the data points of *Bleil* [1973]. The dash-dotted curve is based on M_s-T measurements; all other curves are based on χ-T measurements.

experiments (see section 3.). Some alleged single-phase samples may have contained small amounts of Ilm_{ss} so that the true Tmt composition was richer in Fe than assumed (see section 5.2.). Such features, which can only be detected through careful examination with the SEM, were probably overlooked in several former studies, in particular in those performed in the sixties and the seventies of the last century.

[60] As discussed in section 5.2., the other essential reason for the scatter of the literature data may be seen in the use of single-phase titanomagnetites with unknown, and possibly variable vacancy concentrations. Our results strongly suggest a positive correlation between T_C and the vacancy concentration at given Ti/Fe value, in principle agreement with *Hauptman* [1974] and *Rahman and Parry* [1978]. However, the span in the T_C values at any given Ti/Fe does not exceed 40 K (Figure 5), i.e., is distinctly smaller than proposed in the former studies.

[61] The third factor that can explain discrepancies between our data and those of the literature is the type of measurement employed to retrieve T_C, i.e., either M_s-T or χ-T measurements. As discussed in section 6.3., M_s-T measurements yield higher T_C values for all titanomagnetite compositions in the range $0.2 < X_{Usp} < 0.8$ (Figure 11). At $0.6 < X_{Usp} < 0.8$ our T_C values obtained from M_s-T curves perfectly match those of *Bleil* [1973] (Figure 12), which are also based on saturation magnetization measurements. At lower X_{Usp}, however, the results of *Bleil* [1973] are at lower T_C values than ours (Figure 12). Our values were measured on Tmts synthesized with Ilm_{ss} at 1300°C, those of *Bleil* [1973] concern single-phase Tmts synthesized either at 1300° or 1100°C. Considering that *Bleil* [1973] employed lower fO_2 conditions than ours for his syntheses at $X_{Usp} < 0.6$, his single-phase Tmts most probably had lower

vacancy concentrations than our Tmts (+Ilm_{ss}) and, consequently, lower T_C values.

8. Summary and Implications for Natural Titanomagnetites

[62] On the basis of our experimental results in the Fe-Ti-O system, we have shown that there are well-defined inverse correlations between the Curie temperature of titanomagnetites and their ulvöspinel end-member content (Table 3), with significant differences between the T_C values obtained from Tmt synthesized at 1300°C either in equilibrium with Ilm_{ss} (max. concentration of cation vacancies) or with Wus (min. concentration of cation vacancies). The T_C values for Tmt synthesized at 1100°C in equilibrium with Ilm_{ss}, which plot between the two 1300°C series (Figure 12), represent a good proxy for basaltic parageneses that were rapidly cooled and not oxidized by deuteric or hydrothermal fluids, i.e., essentially for Tmt in submarine pillows and lavas flows. Our calibration curve for 1100°C could represent an upper limit for the T_C values, because natural Tmts may have lower vacancy concentrations, in particular if they reequilibrated at lower temperatures in rocks devoid of Ilm_{ss}. Nonmagnetic elements such as Mg or Al in natural Tmts are also expected to lower the Curie temperature [e.g., *Richards et al.*, 1973; *O'Donovan and O'Reilly*, 1977; *Özdemir and O'Reilly*, 1978, 1981; *Moskowitz*, 1993]. Preliminary own results on Mg- and Al-bearing titanomagnetites, however, confirm that in concentrations relevant to basalts the lowering effect is only slight. Furthermore, natural Tmts were most likely not as rapidly quenched as in the laboratory, that is, their cation distributions may be more ordered than those of our synthetic samples, resulting in reversible χ-T curves with slightly higher T_C values corresponding to those derived from our cooling branches. Indeed, χ-T curves of natural Tmts in submarine basalts, are commonly reversible, if measured in Ar flow [e.g., *Kontny et al.*, 2003; *Vahle and Kontny*, 2005].

[63] In total, our calibration curve for Tmts synthesized at 1100°C in equilibrium with Ilm_{ss} should yield good estimates of the Tmt composition from Curie temperatures in the range 250 to 600 K. For higher T_C values, we recommend the regression curve obtained for Tmts synthesized at 1300°C in equilibrium with Ilm_{ss} (Table 3), because we have no data from samples synthesized at 1100°C with Xusp < 0.4.

[64] Since we have shown that M_s-T measurements yield higher T_C values than χ-T measurements, for Tmt compositions with $X_{Usp} > 0.2$, we recommend not to use calibration curves based on M_s-T measurements [e.g., *Bleil*, 1976; *Bleil and Petersen*, 1982, p.330; *Clark*, 1997; *Hunt et al.*, 1995] to estimate Tmt compositions from T_C retrieved from χ-T measurements. These calibration curves yield overestimates of the ulvöspinel content of titanomagnetites in the range $0.5 < X_{Usp} < 1.0$. With the equation given by *Bleil and Petersen* [1982], the overestimate is of about 0.05, i.e., 5 mol% of the ulvöspinel content (Figure 12). Admittedly, this is not a very strong effect.

[65] In fact, the main uncertainty in estimating the composition of natural Tmts from their Curie temperature stems from the method used to retrieve T_C from the χ-T curves (peak versus intersecting tangents method), as already mentioned by *Petrovsky and Kapicka* [2005]. The χ-T curves reported for Tmt in submarine pillow basalts commonly show a gradual decay of χ around T_C, which reflects the chemical inhomogeneities within and among the titanomagnetite crystals [e.g., *Kontny et al.*, 2003; *Vahle and Kontny*, 2005]. As an example, we may quote sample SR0800-0.9 [*Vahle and Kontny*, 2005] from a massive basaltic pillow (HSDP-2 drill hole in Hawaii), which yields a χ-T curve with a peak at 301 K and a gradual drop of susceptibility, ending at 833 K. With our regression curve for Tmt synthesized in equilibrium with Ilm_{ss} at 1100°C (polynom 4 in Table 3), we obtain a X_{Usp} value of 0.74 from the peak T_C, which should represent the Ti-richest and dominating Tmt composition in the sample. EMP analyses yield, in excellent agreement, a maximum X_{Usp} of 0.75 (C. Vahle, personal communication, 2006) (X_{Usp} value calculated after *Stormer* [1983]). *Vahle and Kontny* [2005] have estimated two T_C values with the intersecting tangents method, one major value at 383 K, and a minor value at 486 K (see their Table 1 and Figure 3a), which would translate into X_{Usp} values of 0.66 and 0.54 with our equation. It is clear that these values represent only rough compositional ''means'' which must not occur in any crystal. In fact, EMP analyses of relatively large Tmt crystals give X_{Usp} values ranging between 0.62 and 0.75. Titanomagnetite crystals that were too small to be analyzed with the EMP are Fe richer.

[66] On the whole, the peak value in a χ-T curve of a titanomagnetite-bearing basalt can yield a reliable estimate of the Tmt composition by using an appropriate regression equation (see Table 3), if all titanomagnetite crystals have very similar compositions. If titanomagnetite is chemically inhomogeneous (i.e., zoned crystals and/or crystals of different compositions over the sample) the peak value from the χ-T curve will give a good estimate of the Ti-richest composition. In contrast, T_C values retrieved with the intersecting tangents method give only approximate mean compositions of the titanomagnetite in the sample.

[67] **Acknowledgments.** The Deutsche Forschungsgemeinschaft (DFG) funded this research through grants La 1164/5-1 and 5-2 within the framework of the International Continental Drilling Program (ICDP). We thank Carsten Vahle (Heidelberg) for help in the rock magnetic laboratory and for discussions, Hans-Peter Meyer for maintenance of the EMP and the SEM, and Ilse Glass and Aleksander Varichev for help at the SEM. Philipp Antrett, Ramona Langner, and Alexandra Vackiner assisted in the laboratories at different stages of the study. We are indebted to David Krása, Jürgen Matzka, and Nikolai Petersen (Munich) for fruitful discussions and assistance during the saturation magnetization measurements. We thank Eduard Petrovsky (Prag) and, especially, Richard Harrison (Cambridge) for their thorough and very helpful reviews and Wyn Williams for his editorial work.

References

Aggarwal, S., and R. Dieckmann (2002), Point defects and cation tracer diffusion in $(Ti_xFe_{1-x})_{3-\delta}O_4$. 1. Non-stoichiometry and point defects, *Phys. Chem. Miner.*, *29*, 695–706.

Akimoto, S. (1954), Thermo-magnetic study of ferromagnetic minerals contained in igneous rocks, *J. Geomagn. Geoelectr.*, *6*, 1–14.

Akimoto, S., T. Katsura, and M. Yoshida (1957), Magnetic properties of $TiFe_2O_4$-Fe_3O_4 system and their change with oxidation, *J. Geomagn. Geoelectr.*, *9*, 165–178.

Aragon, R., and R. H. McCallister (1982), Phase and point defect equilibria in the titanomagnetite solid solution, *Phys. Chem. Miner.*, *8*, 112–120.

Bleil, U. (1971), Cation distribution in titanomagnetites, *Z. Geophys.*, *37*, 305–319.

Bleil, U. (1973), Synthese von Mischkristallen der Titanomagnetit-Reihe und Untersuchungen ihrer für Probleme des Gesteins- und Paläomagne-

tismus wichtigen Kenngrößen, dissertation, 170 pp., Ludwig Maximilian Univ., Munich, Germany.
Bleil, U. (1976), An experimental study of the titanomagnetite solid solution series, *Pure Appl. Geophys.*, *114*, 165–175.
Bleil, U., and N. Petersen (1982), Magnetic properties of natural minerals, in *Numerical Data and Functional Relationships in Science and Technology, Group V: Geophysics and Space Research*, edited by G. Angenheister, pp. 308–365, Springer, New York.
Bücker, C., A. Schult, W. Bloch, and S. D. C. Guerreiro (1986), Rock magnetism and paleomagnetism of an Early Cretaceous/Late Jurassic dike swarm in Rio Grande do Norte, Brasil, *J. Geophys.*, *60*, 129–135.
Buddington, A. F., and D. H. Lindsley (1964), Iron-titanium oxide minerals and synthetic equivalents, *J. Petrol.*, *5*, 310–357.
Calvo, M., M. Prévot, M. Perrin, and J. Riisager (2002), Investigating the reasons for the failure of palaeointensity experiments: A study on historical lava flows from Mt. Etna (Italy), *Geophys. J. Int.*, *149*, 44–63.
Chevallier, R., J. Bolfa, and S. Mathieu (1955), Titanomagnétites et ilménites ferromagnétiques: Étude optique radiocristallographique chimique, *Bull. Soc. Fr. Mineral. Cristallogr.*, *128*, 307–346.
Cisowski, S. (1980), The relationship between the magnetic properties of terrestrial igneous rocks and the composition and internal structure of their component Fe-oxide grains, *Geophys. J.R. Astron. Soc.*, *60*, 107–122.
Clark, D. A. (1997), Magnetic petrophysics and magnetic petrology: aids to geological interpretation of magnetic surveys, *J. Aust. Geol. Geophys.*, *17*(2), 83–103.
Deines, P., R. H. Nafziger, G. C. Ulmer, and E. Woermann (1974), Temperature-oxygen fugacity tables for selected gas mixtures in the system C-H-O at one atmosphere total pressure, *Bull. Earth Min. Sci. Explor.*, *88*, 129 pp.
Deutsch, E. R., R. R. Pätzold, and C. Radhakrishnamurty (1981), Apparent superparamagnetic behavior of some coarse-grained synthetic titanomagnetite, *Phys. Earth Planet. Inter.*, *26*, 27–36.
De Wall, H., A. Kontny, and C. Vahle (2004), Magnetic susceptibility zonation of the melilititic Riedheim dyke (Hegau volcanic field, Germany): Evidence for multiple magma pulses?, *J. Volcanol. Geotherm. Res.*, *131*, 143–163.
Dieckmann, R. (1982), Defects and cation diffusion in magnetite (IV): Nonstoichiometry and point defect structure of magnetite ($Fe_{3-\delta}O_4$), *Ber. Bunsenges. Phys. Chem.*, *86*, 112–118.
Dunlop, D. J., and Ö. Özdemir (1997), *Rock Magnetism*, 573 pp., Cambridge Univ. Press, New York.
Gonzalez, S., G. Sherwood, H. Böhnel, and E. Schnepp (1997), Paleosecular variation in Central Mexico over the last 30000 years: the record from lavas, *Geophys. J. Int.*, *130*, 201–219.
Grommé, C. S., T. L. Wright, and D. L. Peck (1969), Magnetic properties and oxidation of iron-titanium oxide minerals in Alae and Makaopuhi lava lakes, Hawaii, *J. Geophys. Res.*, *74*, 5277–5293.
Haggerty, S. E. (1991), Oxide textures: A mini-atlas, in *Oxide Minerals: Petrologic and Magnetic Significance*, *Rev. Mineral.*, vol. 25, edited by D. H. Lindsley, pp. 129–137, Mineral. Soc. of Am., Washington, D. C.
Harrison, R. J., and A. Putnis (1996), Magnetic properties of the magnetite-spinel solid solution: Curie temperatures, magnetic susceptibilities, and cation ordering, *Am. Mineral.*, *81*, 375–384.
Harrison, R. J., and A. Putnis (1999a), Determination of the mechanism of cation ordering in magnesioferrite ($MgFe_2O_4$) from the time- and temperature-dependence of magnetic susceptibility, *Phys. Chem. Miner.*, *26*, 322–332.
Harrison, R. J., and A. Putnis (1999b), The magnetic properties and crystal chemistry of oxide spinel solid solution, *Surv. Geophys.*, *19*, 461–520.
Hauptman, Z. (1974), High temperature oxidation, range of non-stoichiometry and Curie point variation of cation deficient titanomagnetite, *Geophys. J.R. Astron. Soc.*, *38*, 29–47.
Hrouda, F. (1994), A technique for the measurement of thermal changes of magnetic susceptibility of weakly magnetic rocks by the CS-2 apparatus and KLY-2 Kappabridge, *Geophys. J. Int.*, *118*, 604–612.
Hunt, C. P., B. M. Moskowitz, and S. K. Banerjee (1995), Magnetic properties of rocks and minerals, in *Rock Physics and Phase Relations, A Handbook of Physical Constants*, *Ref. Shelf*, vol. 3, edited by T. J. Ahrens, pp. 189–204, AGU, Washington, D. C.
Ishikawa, Y., N. Nato, and Y. Syono (1971), Neutron and magnetic studies of a single crystal of Fe_2TiO_4, *Tech. Rep. Inst. Solid State Phys. Univ. Tokyo, Ser. A*, *455*.
Ishikawa, Y., N. Saito, M. Arai, Y. Watanabe, and H. Takei (1985), A new oxide spin glass system of $(1-x)FeTiO_3 - xFe_2O_3$.I. Magnetic properties, *J. Phys. Soc. Jpn.*, *54*(1), 312–325.
Jensen, S. D., and P. N. Shive (1973), Cation distribution in sintered titanomagnetites, *J. Geophys. Res.*, *78*, 8474–8480.
Kakol, Z., J. Sabol, and J. M. Honig (1991), Cation distribution and magnetic properties of titanomagnetites $Fe_{3-x}Ti_xO_4$ ($0 \leq x < 1$), *Phys. Rev. B*, *43*, 649–654.
Kontny, A., C. Vahle, and H. de Wall (2003), Characteristic magnetic behavior of subaerial and submarine lava units from the Hawaiian Scientific Drilling Project, *Geochem. Geophys. Geosyst.*, *4*(2), 8703, doi:10.1029/2002GC000304.
Lattard, D. (1995), Experimental evidence for the exsolution of ilmenite from titaniferous spinel, *Am. Mineral.*, *80*, 968–981.
Lattard, D., U. Sauerzapf, and M. Käsemann (2005), New calibration data for the Fe-Ti oxide thermo-oxybarometers from experiments in the Fe-Ti-O system at 1 bar, 1000–1300°C and a large range of oxygen fugacities, *Contrib. Mineral. Petrol.*, *149*, 735–754.
Leonhardt, R. (2006), Analyzing rock magnetic measurements: The RockMagAnalyzer 1.0 software, *Comput. Geosci.*, *32*, 1420–1431.
Lindsley, D. H. (1981), Some experiments pertaining to the magnetite-ulvöspinel miscibility gap, *Am. Mineral.*, *66*, 759–762.
Lindsley, D. H. (1991), Experimental studies of oxide minerals, in *Oxide Minerals: Petrologic and Magnetic Significance*, *Rev. Mineral.*, vol. 25, edited by D. H. Lindsley, pp. 69–106, Mineral. Soc. of Am., Washington, D. C.
Matzka, J., D. Krása, T. Kunzmann, A. Schult, and N. Petersen (2003), Magnetic state of 10–40 Ma old ocean basalts and its implications for natural remanent magnetisation, *Earth Planet. Sci. Lett.*, *206*, 541–553.
Miranda, J. M., P. F. Silva, N. Lourenco, B. Henry, R. Costa, and Saldanha Team (2002), Study of Saldanha Massif (MAR, 36°34′N): Constraints from rock magnetic and geophysical data, *Mar. Geophys. Res.*, *23*, 299–318.
Moskowitz, B. M. (1981), Methods for estimating Curie temperatures of titanomagnetites from experimental J_s-T-data, *Earth Planet. Sci. Lett.*, *53*, 84–88.
Moskowitz, B. M. (1987), Towards resolving the inconsistencies in characteristic physical properties of synthetic titanomaghemites, *Phys. Earth Planet. Inter.*, *46*, 173–183.
Moskowitz, B. M. (1993), High-temperature magnetostriction of magnetite and titanomagnetite, *J. Geophys. Res.*, *98*, 359–371.
Moskowitz, B. M., M. Jackson, and C. Kissel (1998), Low-temperature magnetic behavior of titanomagnetites, *Earth Planet. Sci. Lett.*, *157*, 141–149.
Néel, L. (1955), Some theoretical aspects of rock magnetism, *Adv. Phys.*, *4*, 191–243.
O'Donovan, J. B., and W. O'Reilly (1977), The preparation, characterization and magnetic properties of synthetic analogues of some carriers of the palaeomagnetic record, *J. Geomagn. Geoelectr.*, *29*, 331–344.
O'Donovan, J. B., and W. O'Reilly (1980), The temperature dependent cation distribution in titanomagnetites, *Phys. Chem. Miner.*, *5*, 235–243.
O'Neill, H. S. C. (1987), Quartz-fayalite-iron and quartz-fayalite-magnetite equilibria and the free energy of formation of fayalite (Fe_2SiO_4) and magnetite (Fe_3O_4), *Am. Mineral.*, *72*, 67–75.
O'Neill, H. S. C. (1988), Systems Fe-O and Cu-O: thermodynamic data for the equilibria Fe-"FeO", Fe-Fe_3O_4, "FeO"-Fe_3O_4, Fe_3O_4-Fe_2O_3, Cu-Cu_2O, and Cu_2O-CuO from emf measurements, *Am. Mineral.*, *73*, 470–486.
O'Neill, H. S. C., and A. Navrotsky (1984), Cation distributions and thermodynamic properties of binary spinel solid solutions, *Am. Mineral.*, *69*, 733–753.
O'Neill, H. S. C., and M. I. Pownceby (1993), Thermodynamic data from redox reactions at high temperatures. I. An experimental and theoretical assessment of the electrochemical method using stabilized zirconia electrolytes, with revised values for the Fe-"FeO", Co-CoO, Ni-NiO and Cu-Cu_2O oxygen buffers, and new data for the W-WO_2 buffer, *Contrib. Mineral. Petrol.*, *114*, 296–314.
O'Reilly, W., and S. K. Banerjee (1965), Cation distribution in titanomagnetites (1-x) Fe_3O_4 − x Fe_2TiO_4, *Phys. Lett.*, *17*(3), 237–238.
Özdemir, Ö. (2000), Coercive force of single crystals of magnetite at low temperatures, *Geophys. J. Int.*, *141*, 351–356.
Özdemir, Ö., and W. O'Reilly (1978), Magnetic properties of monodomain aluminium-substituted titanomagnetite, *Phys. Earth Planet. Inter.*, *16*, 190–195.
Özdemir, Ö., and W. O'Reilly (1981), High-temperature hysteresis and other magnetic properties of synthetic monodomain titanomagnetites, *Phys. Earth Planet. Inter.*, *25*, 406–418.
Ozima, M., and E. E. Larson (1970), Low- and high-temperature oxidation of titanomagnetite in relation to irreversible changes in the magnetic properties of submarine basalts, *J. Geophys. Res.*, *75*, 1003–1017.
Petrovsky, E., and A. Kapicka (2005), Comments on "The use of field dependence of magnetic susceptibility for monitoring variations in titanomagnetite composition: A case study on basanites from the Vogelsberg 1996 drillhole, Germany" by de Wall and Nano, Stud. Geophys. Geod., 48, 767–776, *Stud. Geophys. Geod.*, *49*, 255–258.

Price, G. D. (1981), Subsolidus phase relations in the titanomagnetite solid solution series, *Am. Mineral.*, *66*, 751–758.

Rahman, A. A., and L. G. Parry (1978), Titanomagnetites prepared at different oxidation conditions: hysteresis properties, *Phys. Earth Planet. Inter.*, *16*, 232–239.

Richards, J. C. W., J. B. O'Donovan, Z. Hauptman, W. O'Reilly, and K. M. Creer (1973), A magnetic study of titanomagnetite substituted by magnesium and aluminium, *Phys. Earth Planet. Inter.*, *7*, 437–444.

Senderov, E., A. U. Dogan, and A. Navrotsky (1993), Nonstoichiometry of magnetite-ulvöspinel solid solutions quenched from 1300°C, *Am. Mineral.*, *78*, 565–573.

Simons, B., and E. Woermann (1978), Iron titanium oxides in equilibrium with metallic iron, *Contrib. Mineral. Petrol.*, *66*, 81–89.

Stephenson, A. (1969), The temperature dependent cation distribution in titanomagnetites, *Geophys. J. R. Astron. Soc.*, *18*, 199–210.

Stephenson, A. (1972), Spontaneous magnetization curves and Curie points of cation deficient titanomagnetites, *Geophys. J. R. Astron. Soc.*, *29*, 91–107.

Stormer, J. C., Jr. (1983), The effects of recalculation on estimates of temperature and oxygen fugacity from analyses of multicomponent iron-titanium oxides, *Am. Mineral.*, *68*, 286–594.

Taylor, R. W. (1964), Phase equilibria in the system FeO-Fe_2O_3-TiO_2 at 1300°C, *Am. Mineral.*, *49*, 1016–1030.

Trestman-Matts, A., S. E. Dorris, S. Kumarakrishnan, and T. O. Mason (1983), Thermoelectric determination of cation distributions in Fe_3O_4-Fe_2TiO_4, *J. Am. Ceram. Soc.*, *66*, 829–834.

Tucker, P. (1981), Low-temperature magnetic hysteresis properties of multidomain single-crystal titanomagnetite, *Earth Planet. Sci. Lett.*, *54*, 167–172.

Vahle, C., and A. Kontny (2005), The use of field dependence of AC susceptibility for the interpretation of magnetic mineralogy and magnetic fabrics in the HSDP-2 basalts, Hawaii, *Earth Planet. Sci. Lett.*, *238*, 110–129.

Vincent, E. A., J. B. Wright, R. Chevallier, and S. Mathieu (1957), Heating experiments on some natural titaniferous magnetites, *Mineral. Mag.*, *31*, 624–655.

Wanamaker, B. J., and B. M. Moskowitz (1994), Effect of nonstoichiometry on the magnetic and electrical properties or synthetic single crystal $Fe_{2.4}Ti_{0.6}O_4$, *Geophys. Res. Lett.*, *21*, 983–986.

Waychunas, G. A. (1991), Crystal chemistry of oxides and oxyhydroxides, in *Oxide minerals: Petrologic and Magnetic Significance*, *Rev. Mineral.*, vol. 25, edited by D. H. Lindsley, pp. 11–68, Mineral. Soc. of Am., Washington, D. C.

Wechsler, B. A., D. H. Lindsley, and C. T. Prewitt (1984), Crystal structure and cation distribution in titanomagnetites ($Fe_{3-x}Ti_xO_4$), *Am. Mineral.*, *69*, 754–770.

Wißmann, S., V. v. Wurmb, F. J. Litterst, R. Dieckmann, and K. D. Becker (1998), The temperature-dependent cation distribution in magnetite, *J. Phys. Chem. Solids*, *59*, 321–330.

Wu, C. C., and T. O. Mason (1981), Thermopower measurement of cation distribution in magnetite, *J. Am. Ceram. Soc.*, *64*, 520–522.

Zhou, W., R. van der Voo, D. R. Peacor, and Y. Zhang (2000), Variable Ti-content and grain size of titanomagnetite as a function of cooling rate in very young MORB, *Earth Planet. Sci. Lett.*, *179*, 9–20.

R. Engelmann, D. Lattard, and U. Sauerzapf, Mineralogisches Institut, Universität Heidelberg, INF 236, D-69120 Heidelberg, Germany. (dlattard@min.uni-heidelberg.de)

A. Kontny, Geologisch-paläontologisches Institut, Universität Heidelberg, INF 234, D-69120 Heidelberg, Germany.